Sensor Fusion and Predictive Control for Adaptive Vehicle Headlamp Alignment: A Comparative Analysis

Glenson Toney [1], Gaurav Sethi [2], Cherry Bhargava [3], Aldrin Claytus Vaz [4], Navya Thirumaleshwar Hegde [5*]
[1, 2] School of Electronics and Electrical Engineering, Lovely Professional University, Phagwara-144411, Punjab, India
[1] Department of Electronics and Communication Engineering, School of Engineering, St Aloysisus (Deemed to be University), Mangaluru-575003, Karnataka, India
[3] Department of Electronics and Telecommunication Engineering, Symbiosis International University, Pune-412115, Maharashtra, India
[4] Department of Electronics and Communication Engineering, St Joseph Engineering College, Visvesvaraya Technological University, Mangaluru-575028, Karnataka, India
[5] Department of Aeronautical and Automobile Engineering, Manipal Institute of Technology, Manipal Academy of Higher Education, Manipal-576104, Karnataka, India
Email: [1] glensherton@gmail.com, [2] gaurav.11106@lpu.co.in, [3] cherry_bhargav@yahoo.co.in, [4] aldrinv@sjec.ac.in, [5] navya.hegde@manipal.edu
*Corresponding Author

Abstract*—Nighttime driving safety is often compromised by the inability of conventional adaptive headlamp systems to account for lateral slip and rapidly changing road conditions, leading to misalignment and reduced visibility during aggressive maneuvers. Most existing approaches rely solely on steering angle, which limits adaptability under dynamic slip scenarios. This study presents the development and comparative evaluation of a Fused Controller that uniquely integrates sensor fusion, adaptive gain scheduling, and multi-step predictive optimization for robust adaptive headlamp alignment. Five control architectures- Filtered Proportional Controller (FPC), Raw State MPC (RS-MPC), Extended MPC (E-MPC), Feedforward-Enhanced MPC (FF-MPC), and the proposed Fused Controller- were systematically evaluated on a 2 km synthetic road with ten challenging segments. Compared to the E-MPC baseline, the Fused Controller achieved a 42.5% reduction in root mean square error (RMSE) in long S-curves and a 30.6% improvement in sharp turns, with a settling time of 0.6 s (versus 1.8 s for FPC) and a jitter index of 9.93°/s. Frequency-domain analysis confirmed a 1.2 Hz bandwidth with actuator-compatible roll-off, and stability analysis validated robustness under noise and disturbances. Statistical analysis across 20 independent simulation runs per controller showed these improvements are highly significant ($p < 0.001$, large Cohen's d), confirming the practical superiority of the Fused Controller. These results indicate enhanced driver visibility and reduced nighttime collision risk, while the controller's computational efficiency and adaptive gains support scalability and real-world deployment. This work provides a rigorous and practical framework for next-generation adaptive lighting systems.

Keywords—Adaptive Headlamps; Headlamp Steering; Inertial Measurement Unit (IMU); Kalman Filter; Nighttime Safety; Slip Angle Estimation; Vehicle Dynamics Control.

Notations

$U(t)$	*: Longitudinal velocity* (m/s)
$V(t)$	*: Lateral velocity* (m/s)
$\Omega(t)$	*: Yaw rate (angular velocity)* (rad/s)
δ	*: Steering angle input (rad)*
θ	*: Vehicle heading angle* (rad)
$\beta(t)$	*: Vehicle slip angle* (rad)
F_x	*: Longitudinal force (N)*
F_{yf}, F_{yr}	*: Lateral forces at front/rear tires (N)*
F_D, F_L	*: Aerodynamic drag/lift forces (N)*
F_{bf}, F_{br}	*: Braking force front/rear (N)*
$C_{\alpha f}, C_{\alpha r}$	*: Tire Cornering stiffness (front/rear)* (N/rad)
μ	*: Coefficient of friction, tire-road*
M	*: Vehicle mass* (kg)
J	*: Yaw moment of inertia* $(kg\ m^2)$
a, b	*: Distance from CG to front/rear axle* (m)
ρ	*: Air density* (kg/m^3)
C_D	*: Aerodynamic drag coefficient*
A	*: Frontal area of vehicle* (m^2)
g	*: Acceleration due to gravity* (m/s^2)
θ_{max}	*: Max allowable headlamp deflection* (rad)
τ	*: Time constant of the headlamp actuator* (s)
T_s	*: Sampling time interval* (s)
α	*: Filter coefficient* $(0 < \alpha < 1)$
C_L	*: Lift coefficient*
C_r	*: Rolling resistance coefficient*
R	*: Wheel radius* (m)
ω	*: Angular speed of wheel* (rad/s)
J_w	*: Rotational inertia of wheel* (kg/m^2)
T_d	*: Driving torque (Nm)*
λ	*: Wheel slip ratio*
$\theta_{HL}(t)$	*: Headlamp deflection angle* (rad)
$\Delta\theta_{HL}[k]$	*: Change in headlamp angle per step (rad)*
k_δ	*: Steering feedback gain*
k_d	*: Headlamp deflection gain*
k_h	*: Proportional gain slip angle to headlamp angle*
k_ψ	*: Proportional gain on road heading to headlamp*
k_{h0}	*: Base value of* k_h
$k_{\psi 0}$	*: Base value of* k_ψ
U_{nom}	*: Nominal speed for gain scaling (m/s)*
$\psi_{road}[k]$	*: Road heading at time step k (rad)*
$\theta_{ref}(t)$	*: Reference Headlamp angle (rad)*
H	*: Prediction horizon*
λ	*: Weight for rate penalty in MPC cost*

γ : *Fusion weighing factor (*$0 < \gamma < 1$)
β_{true} :*True slip angle (rad)*
β_{model} :*Model-based slip angle (rad)*
β_{est} : *Estimated slip angle (rad)*
Ω_{true} :*True yaw rate (rad/s)*
Ω_{model} :*Model-based yaw rate (rad/s)*
Ω_{est} : *Estimated yaw rate (rad/s)*

I. INTRODUCTION

Night time driving safety is fundamentally constrained by the ability of headlamp systems to accurately illuminate the vehicle's true path, especially during dynamic maneuvers where lateral slip causes deviations between steering input and actual trajectory [1]-[3]. Conventional steering-angle-based systems fail under hard cornering, low-traction conditions, or emergency maneuvers, where slip angle (β)—the angular difference between a vehicle's velocity vector and longitudinal axis—becomes critical for adaptive headlamp alignment [4]-[7]. Most current adaptive lighting systems are limited by their reliance on steering angle alone, which does not account for real-time vehicle dynamics or slip, leading to frequent misalignment and compromised visibility in challenging scenarios. Quantitatively, such systems exhibit higher tracking error, directly impacting nighttime accident risk.

Advanced control strategies, such as Filtered Proportional Control (FPC) and Model Predictive Control (MPC), address these limitations by integrating real-time vehicle dynamics, road geometry anticipation, and sensor fusion [6][7]. The slip angle has proven to be a reliable predictor of vehicle trajectory, with prediction errors as low as 0.3 meters, achieved through comprehensive dynamic vehicle modeling. This model incorporates nonlinear equations for longitudinal, lateral, and yaw motions, tire force characteristics, rolling resistance, aerodynamic effects, and load transfer during braking and acceleration [10]-[12]. These enable real-time computation of β from measured or estimated vehicle states, forming the core of modern adaptive headlamp control strategies [2][3].

Recent research has explored slip angle estimation, predictive control, and sensor fusion for improved vehicle dynamics control [7]. However, existing adaptive headlamp solutions rarely integrate these methods holistically, and often neglect computational efficiency or real-time deployability on automotive-grade hardware. The specific scientific problem addressed in this research is the lack of an integrated, real-time control architecture for adaptive headlamp alignment that can robustly compensate for lateral slip, actuator constraints, and transient road conditions.

A foundational approach, the Filtered Proportional Controller (FPC), maps the estimated slip angle to headlamp deflection via a low-pass filtered proportional law [2][3][8][9]. While effective in damping high-frequency noise and ensuring smooth transitions, FPC remains reactive and susceptible to steady-state errors during rapid curvature changes. To overcome these limitations, predictive control strategies like Raw State MPC (RS-MPC) align headlamp direction with projected road heading but lack feedback from dynamic vehicle states, leading to instability under sensor noise [2][3], [10]-[12]. The Extended MPC (E-MPC) addresses this by incorporating slip angle and yaw rate into the optimization framework, improving transient response and robustness. However, E-MPC's reactive nature limits performance in rapidly changing curvature conditions. The Feedforward-Enhanced MPC (FF-MPC) integrates road curvature preview with slip feedback, reducing latency by 30% in simulated S-curve [1], [10]-[12].

Despite these advancements, there remains a gap in synergistically combining sensor fusion, adaptive gain scheduling, and predictive optimization for adaptive headlamp control [4]-[7], [10]-[12]. The research contribution is the development and comparative evaluation of a Fused Controller that uniquely integrates sensor fusion (via Kalman-filtered IMU data), adaptive gain scheduling, and multi-step predictive optimization for robust, real-time adaptive headlamp alignment. By merging real-time inertial measurement unit (IMU) data with model-predicted slip dynamics, the controller achieves reduction in root mean square error (RMSE) compared to E-MPC in 2 km multi-segment trials. The key innovations include:

- A dynamic vehicle model integrating longitudinal, lateral, and yaw dynamics with tire force nonlinearities and aerodynamic effects.
- A sensor-fused predictive framework combining road curvature anticipation with adaptive gains scaled to vehicle speed.
- Actuator-aware smoothing via first-order lag compensation, ensuring mechanical feasibility and visual continuity.

This paper is structured to first introduce the significance of slip angle in vehicle dynamics and its role in headlamp alignment, followed by mathematical modeling, controller design, and a comprehensive segment-wise comparative evaluation of five controllers: Filtered Proportional Controller (FPC), Raw State MPC (RS-MPC), Extended MPC (E-MPC), Feedforward-Enhanced MPC (FF-MPC), and the proposed Fused Controller. A dedicated section presents the statistical analysis of all key performance metrics, including confidence intervals, p-values, and effect sizes, to rigorously validate the comparative results. The findings demonstrate the practical and theoretical advantages of the proposed Fused Controller, establishing a new benchmark for adaptive lighting systems in both conventional and autonomous vehicles.

II. LITERATURE

Adaptive Front-lighting Systems (AFS) are needed to enhance the safety of night driving by changing the direction of the headlamp beam dynamically as a function of vehicle motion. Multiple studies emphasized the crucial role of AFS in better illuminating roadways during turning and reducing visual lag in reduced-light driving conditions [1]. Analysis has demonstrated shortcomings of conventional fixed headlights and proposed detection-based adjustments as a safer alternative [2][3]. Mechanical solutions were shown through designs integrating steering-based control, which ensured efficient beam direction without reliance on complex electronics [4]-[7]. Significant improvement was gained in

AFS reaction time and accuracy. A study created a beam control architecture using road curvature and geometric constraint, leading to improved seeing distance through swiveling mechanisms [8][9]. Another study explored 3D simulation models that examined the effectiveness of headlight alignment with respect to highway geometry [10]-[12]. Parallel efforts led to cost-effective, sensor-based systems using ultrasonic and accelerometer modules for real-time beam control [13]. The industry witnessed growth in microcontroller-controlled AFS devices meant to provide greater visibility under fog or sharp-curve conditions [9]. A mechanical redesign integrated these enhancements and proposed modular upgrades to enhance their range and angular versatility [14]. The necessity of a revolving beam design for turn anticipation and fog navigation, particularly in undulating terrain was discussed [15][16]. In summary, cost-effective prototypes with rack-and-pinion systems were found to offer efficient AFS solutions for cars in emerging economies [18]. The early installations of Adaptive Front-lighting Systems (AFS) were largely based on steering angle as the primary control input to headlamp position. These systems assumed a linear relationship between road curvature and steering wheel angle, giving a straightforward approach for beam alignment while cornering. A steering control prototype was designed, with feedback mechanisms to adjust beam intensity and deflection angle based on real-time road geometry and speed changes [19]. A analytical study brought further improvements by categorizing control techniques into mechanically linked, servo-based, and electronically actuated systems, highlighting the trade-offs in accuracy and responsiveness [20].

Rack-and-pinion linkage systems have gained popularity because they can easily be retrofitted onto current vehicles, as discussed in a number of mechanical design researches [21], [22]. The approach discussed in [23] used a gear motor-driven control approach to ensure reliable beam tracking in tight urban curves, while another study applied simple gear mechanisms connected to the steering column to enhance visibility in turns [24]. Also targeted was beam spread, where feedback from the steering column enabled improvement of lit spaces, particularly on curved roads [25]. Current deployments consider integration of object detection systems to enhance adaptive control logic in real-world situations [26]-[29], with optimization models evaluating beam performance under different driving conditions [30][31]. Steering wheel angle-based trajectory alignment was supplemented by algorithmic beam projection control models to achieve better dynamic performance and fault tolerance during low-speed operations [32]-[36]. Steering-angle-based AFS systems are inexpensive and straightforward but have problems with situations involving vehicle dynamics such as lateral slip or understeer that decouple real motion from steering intent. The lack has spurred increased research interest in the use of vehicle body dynamics—specifically slip angle—as a more stable control input. Steering-angle-based headlamp systems offer a basic correlation between driver input and beam direction, though generally fail to account for vehicle dynamics during aggressive maneuvers or low-friction conditions. Here, the slip angle—defined as the angular difference between the direction of a vehicle and the resulting path—is a more accurate description of vehicular dynamics, making it a relevant parameter to adaptive control systems. Estimation of slip angle was originally underscored as a key role in pioneering research utilizing a nonlinear observer to estimate sideslip and tire forces with inclusion of cornering stiffness to enhance accuracy [37]. This approach laid the groundwork for later algorithms that simultaneously considered yaw rate and sideslip angle, the core of modern vehicle stability systems [38]. Later developments led to more advanced observer-based systems for slip estimation, including experimental verification on instrumented test vehicles [39]. Simultaneous research efforts applied the Extended Kalman Filter (EKF) to combine noisy sensor readings with accurate slip estimations under varied road and load conditions [40]. An important advancement occurred with the inclusion of machine learning techniques, where deep neural networks were integrated along with vehicle sensor data to predict sideslip angle in extremely nonlinear environments [41]-[44].

Hybrid systems using Radial Basis Function (RBF) neural networks combined with Unscented Kalman Filters (UKF) have displayed improved estimation capability under transient conditions [45]. Artificial Neural Networks (ANN) based methods that were tested on empirical vehicle dynamic data significantly reduced dependency on the direct measurement of lateral acceleration and wheel speeds [46]. One particularly innovative contribution was the UKF-informed neural estimating model, which achieved better filtering of dynamic noise through learnt priors [47]. Recent advances have delivered hybrid learning models that address both epistemic and aleatoric uncertainty in slip angle estimation. These models integrated traditional physics-based formulations with probabilistic neural networks, leading to accurate slip predictions across a wide range of vehicle speeds and road conditions. A strong hybrid observer was implemented, combining model-based prediction with neural output to achieve notable immunity to sensor noise and actuator delay [49]. The development of these estimation techniques forms a strong foundation for adding slip angle as a control variable to headlamp systems. This enables anticipatory beam deflection in accordance with the real vehicle path instead of just steering input, thus overcoming limitations of classical AFS systems. Model Predictive Control (MPC) has emerged as a flexible method for controlling vehicle dynamics within constraints, especially for path following and advanced driver-assistance systems. Its predictive nature, ability to control multi-variable systems, and built-in constraint management make it particularly suitable for real-time automotive use. A detailed review of Model Predictive Control (MPC) applications in autonomous driving integrated different prediction models, control structures, and solver settings used for vehicle path tracking [50][51]. A dedicated path tracking controller was suggested for autonomous vehicles, using steering dynamics to provide real-time lane-keeping and trajectory following. Low-speed navigation challenges were addressed through the introduction of dynamic hybrid linear-nonlinear Model Predictive Control systems that adapted to changing road curvature, thus enhancing control robustness in urban settings [52].

Researchers have also discussed the wide scope of automobile Model Predictive Control (MPC) from its inception as a theoretical idea to embedded implementation, while acknowledging the computational overhead and real-time constraints of practical limitations [53]. There is a specific body of research that focuses on autonomous ground vehicles, including combined route and speed tracking methods based on Model Predictive Control frameworks for coordinated actuator control [54]. In high-performance applications such as autonomous racing, tube-based Model Predictive Control (MPC) models showed reliable performance under conditions of model uncertainties and aggressive driving [55]. For enabling tighter integration with actuator systems, time-varying linear model predictive control (LTV-MPC) methods were created and empirically verified on active steering testbeds, displaying high-frequency stability and improved transient responsiveness [56]. Similarly, smooth trajectory generation taking actuator dynamics into account was achieved through limited Model Predictive Control (MPC) frameworks that prevented abrupt steering commands while ensuring lane keeping [57]. Apart from the conventional Model Predictive Control (MPC) formulations, there have emerged control methods such as Robust Model Predictive Path Integral Control (MPPI) that offer a probabilistically rooted alternative with mathematical performance guarantees in stochastic environments [58]. Lastly, predictive control techniques have been extended to lateral vehicle dynamics, enabling application to synchronized cornering and stabilization of drift through bounded trajectory optimization [59]. These studies affirm the importance of Model Predictive Control (MPC) as an essential method in intelligent vehicle control, providing a basis for its adoption into adaptive headlamp systems, especially when complemented by slip angle estimates and dynamic preview capabilities. The efficiency of adaptive vehicle control systems relies on the accuracy and timeliness of dynamic state estimates. Sensor fusion, especially in conjunction with filtering algorithms like the Kalman filter, has seen widespread use for recovering accurate vehicle state data such as slip angle, yaw rate, and lateral acceleration from delayed, noisy, or missing sensor information. Initial attempts at distributed Kalman filtering for vehicular networks addressed data transmission delays by providing fusion algorithms with finite-time convergence to improve estimation accuracy under real-time conditions [60]. Parallel efforts explored adaptive navigation filters that combined model-based and learning-based approaches, enabling real-time covariance adaptation according to changing driving conditions [61]. In high-dimensional estimation, Kalman structures such as DeepUKF, enriched with deep learning, have provided improved stability in vision-inertial navigation through adaptive combination of visual and inertial modalities [62].

Multi-modal sensor fusion methods employing the Extended Kalman Filter (EKF) were developed and validated for autonomous high-speed operation on racing vehicles and proved to be robust in aggressive maneuvers [63][64]. Comprehensive surveys outlined taxonomies of multi-sensor fusion techniques across vehicular domains, emphasizing the value of consensus filtering, distributed data association, and mode switching to improve redundancy and fault tolerance [65]. Ground-breaking work on the integration of inertial sensors with GPS observation for sideslip and roll rate estimation laid the groundwork for vehicle sensor fusion techniques now accepted as de facto [66]. A head-to-head comparison of EKF and UKF approaches to GPS/INS fusion illustrated the compromises between estimation robustness and computational complexity, offering critical insights for controller design under resource constraints [67]. Real-time applications of these fusion algorithms have been proven as reference systems for vehicle navigation, confirming their applicability in real-world environments [68]. Follow-up analyses assessed the performance of MEMS-based integration, highlighting its tunability with filter sensitivity and noise modeling [69]. Sensor fusion algorithms were finally rigorously tested through flight tests for attitude estimation, bridging terrestrial vehicle dynamics with aerospace-quality estimate approaches [70]. These work-pieces emphasize the critical role of sensor fusion in transforming raw vehicle sensor data into actionable control inputs. They are the basis for advanced control systems—like adaptive headlamp controllers—where accurate and timely vehicle alignment and slip evaluation are vital to safety and performance. Despite significant developments in vehicle dynamics, predictive control, and adaptive systems, substantial boundaries remain in the area of adaptive headlamp control based on dynamic vehicle behavior. There is a large gap in research on integrating slip angle calculation into headlamp control systems. While accurate methods of sideslip detection have been devised for stability control and path tracking, their use in beam deflection and road illumination remains insufficiently explored [71].

Further, while Kalman-based predictive filtering is common in navigation and estimating schemes, its use for beam lobe control—particularly under transient conditions—remains limited [72]. The research is lacking in adaptive gain scheduling algorithms for beam control that compensate based on real-time variables such as speed and lateral acceleration, although they have proven to be effective in more comprehensive vehicle control systems [73]. Despite significant improvement in observer-based estimation and sensor integration methods, their potential to enhance beam alignment in low visibility and cornering modes in lighting control is still not fully tapped [74]. While Model Predictive Control (MPC) has emerged as a core methodology in lateral vehicle dynamics and path optimization, its realization in adaptive headlights is rare. Sparse solutions combine anticipatory road preview, slip compensations, or beam actuator limits into a single MPC framework [75]. In addition, most published work does not conduct segment-specific tests of beam effectiveness over complex road geometries, such as acute turns, S-curves, or zigzags [76]. The computational feasibility of deploying complex controllers—like Model Predictive Control (MPC) or combined slip estimators—on car-grade embedded systems is not adequately explored. This limits the application of research-grade models to commercially acceptable applications [77]. Additionally, environmental dynamics, like changing road friction and weather-induced surface irregularities, are usually excluded from beam control reasoning, even though they directly affect tire performance and path prediction [78][79]. Computer simulation validated over different road geometries and real-

time constraints is the focus of this research, unlike earlier research that called for Hardware-in-the-Loop (HIL) testing in order to measure real-time control performance. Lastly, the headlamp assembly's actuator dynamics, including mechanical limits, rate limits, and potential backlash, are often neglected, even though they contribute to slowing beam response in high-speed transitions [80][81]. Despite advancements in slip angle estimation, predictive control, and sensor fusion, a cohesive architecture that couples these into a deployable, real-time lighting solution remains unachieved. Existing models often address isolated aspects of the problem but fail to capture the complex, nonlinear relationships between vehicle trajectory, environmental reaction, and actuator performance. This fragmentation underscores the pressing need for an integrated control framework—one that is predictive, adaptive, and computationally efficient. This paper introduces a fused controller that leverages dynamic vehicle modeling, real-time filtering, and anticipatory optimization to enhance beam alignment for enhanced nighttime safety and autonomous readiness.

III. METHODOLOGY

This section details the systematic development of five control architectures for adaptive headlamp alignment: Filtered Proportional Controller (FPC), Raw State MPC (RS-MPC), Extended MPC (E-MPC), Feedforward-Enhanced MPC (FF-MPC), and the Fused Control Model. These controllers were chosen to represent a spectrum of design philosophies—from simple reactive to advanced predictive and sensor-fused strategies—reflecting both the state of the art and practical constraints in automotive lighting control. The selection ensures coverage of both baseline and advanced methods, enabling a comprehensive evaluation of trade-offs in robustness, computational feasibility, and real-world applicability. Dynamic vehicle modeling, predictive optimization, and sensor fusion are integrated (Table I) to ensure robust beam alignment under diverse driving conditions. A detailed flowchart (Fig. 1) summarizes the research methodology, from vehicle modeling and controller design to simulation and performance evaluation.

A. Dynamic Vehicle Modeling

A nonlinear vehicle dynamics model forms the foundation for real-time slip angle (β) estimation. The model incorporates longitudinal, lateral, and yaw motions, tire force characteristics, aerodynamic effects, and load transfer. This modeling approach is widely accepted for its balance of fidelity and computational efficiency in automotive control applications [37]–[40], [50], [53] and is represented using equations (1) through (4).

TABLE I. ALGORITHM FOR THE CONTROLLERS (FPC, R-MPC, E-MPC, FF-MPC AND F-CONTROLLER)

A. Filtered Proportional Controller	B. Raw Full-State MPC with Direct Road Heading Injection	E. Fused Controller
1: Initialize: Time constant τ, proportional gain k_h, sampling time T_s 2: for each control update do 3: Measure slip angle $\beta[k]$ 4: Calculate filter coefficient α 5: Update $\theta_{HL}[k]$ 6: Apply saturation: $\theta_{HL}[k] \epsilon\ [-\theta_{max}, \theta_{max}]$ 7: Apply control input $\theta_{HL}[k]$ 8: end for	1: Initialize: Predictive horizon N, weight λ 2: for each control update do 3: Measure road heading $\psi_{road}[k]$ 4: Predict future road heading $\psi_{road}[k+i]$ over N steps 5: Solve optimization problem: Minimize L 6: Obtain optimal θ_{HL} sequence 7: Apply first control input $\theta_{HL}[k]$ 8: Apply saturation: $\theta_{HL}[k] \epsilon\ [-\theta_{max}, \theta_{max}]$ 9: end for	1: Initialize: Short-term gains k_Ω, k_β blending parameter γ, multi-step horizon N, velocity-dependent gains $k_\Omega(U), k_\beta(U)$ weighting factor w 2: for each control update do 3: Measure true yaw rate $\Omega_{true}[k]$, slip angle $\beta_{true}[k]$ vehicle velocity $U[k]$, and states 4: Estimate model-based yaw rate and slip angle 5: Predict one step ahead values $\Omega_{pred}[k]$ and $\beta_{pred}[k]$ 6: Calculate short-term control $\theta_{HL}^{short}[k]$ 7: Predict future yaw rates and slip angles over N steps 8: Calculate average future values: $\bar{\Omega}_{future}$ and $\bar{\beta}_{future}$ 9: Update velocity-dependent gains based on current velocity 10: Calculate long-term control $\theta_{HL}^{long}[k]$ 11: Combine control strategies $\theta_{HL}[k]$ 12: Apply low-pass filter to reduce jitter 13: Apply saturation: $\theta_{HL}[k] \epsilon\ [-\theta_{max}, \theta_{max}]$ 14: Apply control input $\theta_{HL}[k]$ 15: end for
C. Extended Model Predictive Controller	D. Feedforward-Enhanced MPC	
1: Initialize: Predictive horizon N, weight λ, state-space matrices A_d, B_d 2: for each control update do 3: Measure current state $x[k]$ 4: Predict future states $x[k+i]$ over N steps using state-space model 5: Extract predicted slip angles $\beta[k+i]$ from predicted states 6: Solve optimization problem: Minimize L 7: Obtain optimal θ_{HL} sequence 8: Apply first control input $\theta_{HL}[k]$ 9: Apply saturation: $\theta_{HL}[k] \epsilon\ [-\theta_{max}, \theta_{max}]$ 10: end for	1: Initialize: Predictive horizon N, weight λ, gains k_h, k_ψ 2: for each control update do 3: Measure slip angle $\beta[k]$ and road heading $\psi_{road}[k]$ 4: Predict future slip angles $\beta[k+i]$ and road headings $\psi_{road}[k+i]$ over N steps 5: Calculate reference angles $\theta_{ref}[k+i]$ 6: Solve optimization problem: Minimize L 7: Obtain optimal θ_{HL} sequence 8: Apply first control input $\theta_{HL}[k]$ 9: Apply saturation: $\theta_{HL}[k] \epsilon\ [-\theta_{max}, \theta_{max}]$ 10: end for	

Longitudinal dynamics:

$$M\dot{U}(t) = F_x - F_D - F_{br} - F_{yr}\sin(\delta) \quad (1)$$

Lateral dynamics:

$$M\dot{V}(t) = F_{yf}\cos(\delta) + F_{yr} - MU(t)\Omega(t) \quad (2)$$

Yaw dynamics:

$$J\dot{\Omega}(t) = aF_{yf} - bF_{yr} \quad (3)$$

The slip angle is computed as:

$$\beta(t) = \tan^{-1}\left(\frac{V(t)}{U(t)}\right) \quad (4)$$

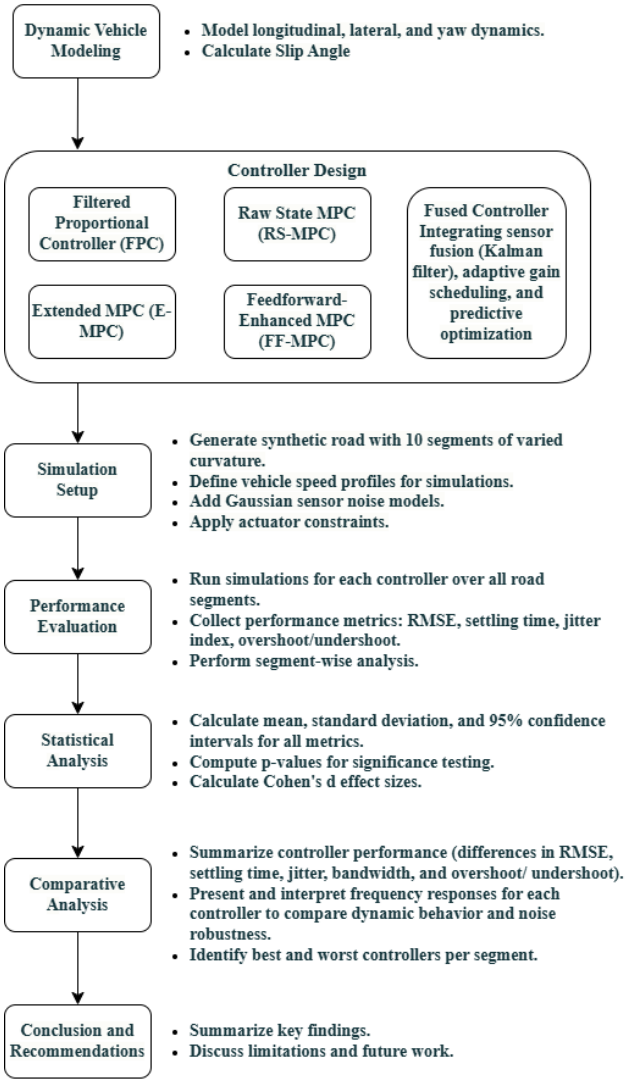

Fig. 1. Flowchart of the research work

B. Controller Design

1) Filtered Proportional Controller (FPC)

The FPC utilizes a low-pass filtered proportional law to relate real-time slip angle to headlight deflection. The use of first-order lag smooths actuator commands and reduces high-frequency noise from vehicle sensors, thus ensuring smooth and comfortable beam transitions. While computationally simple and robust in most conditions, it is reactive in nature and tends to show steady-state faults during rapid directional changes. FPC maps $\beta(t)$ to headlamp deflection $\theta_{HL}(t)$ via a low-pass filtered proportional law as shown in equations (5) through (7).

Continuous-time:

$$\tau\dot{\theta}_{HL}(t) + \theta_{HL}(t) = k_h\beta(t) \quad (5)$$

Discrete-time implementation:

$$\theta_{HL}[k] = \alpha\theta_{HL}[k-1] + (1-\alpha)k_h\beta[k], \alpha = \frac{\tau}{\tau + T_s} \quad (6)$$

Actuator constraints:

$$\theta_{HL}(t) \in [-\theta_{\max}, \theta_{\max}] \quad (7)$$

2) Raw State MPC (RS-MPC)

RS-MPC aligns the headlamp direction with the predicted road path by minimizing the difference between headlamp deflection and the target road path (Equation (8)). It does not have dynamic vehicle feedback, (slip angle and yaw rate), making it simple but prone to noise and prediction errors in road curvature. The lack of feedback limits its robustness in transient or highly dynamic maneuvers. RS-MPC aligns headlamps with road heading (ψ_{road}) without slip feedback.

Cost function:

$$\min_{\theta_{HL}} \sum_{k=0}^{N} (\theta_{HL}[k] - \psi_{road}[k])^2 + \lambda(\Delta\theta_{HL}[k])^2 \quad (8)$$

subject to $|\theta_{HL}[k]| \leq \theta_{max}$, $|\Delta\theta_{HL}[k]| \leq \delta_{max}$

3) Extended MPC (E-MPC)

E-MPC includes slip angle and yaw rate within an optimization-based predictive framework, using a state-space vehicle model to predict future vehicle states. It adjusts headlamp deflection dynamically to track slip angle trends while respecting actuator constraints as represented by equations (9) through (11). E-MPC improves transient response and noise robustness compared to less complex controllers; however, it is still largely reactive and does not have direct foresight of road geometry.

E-MPC integrates slip angle and yaw dynamics into a state-space predictive framework:

State vector:

$$x[k] = [\beta[k]\ \Omega[k]]^T \quad (9)$$

Discrete-time model:

$$x[k+1] = A_d x[k] + B_d\delta[k] \quad (10)$$

derived via Euler discretization of continuous dynamics.
Cost function:

$$\min_{\theta_{HL}} \sum_{k=0}^{N} (\theta_{HL}[k] - k_h\beta[k])^2 + \lambda(\Delta\theta_{HL}[k])^2 \quad (11)$$

4) Feedforward-Enhanced MPC (FF-MPC)

FF-MPC combines slip angle feedback with a feedforward element based on real-time road heading estimates. The combined strategy allows for anticipatory beam adjustments for upcoming road curvatures, reducing delay and increasing tracking accuracy. A filtered actuator model ensures smooth switch-ons. FF-MPC shows

excellence in scenarios involving complex or rapidly varying trajectories as shown in equations (12) and (13); however, it can be limited by static gain values.

FF-MPC combines road curvature preview with slip feedback:

Reference angle:

$$\theta_{\text{ref}}(t) = k_h\beta(t) + k_\psi\psi_{\text{road}}(t) \quad (12)$$

First-order actuator model:

$$\dot{\theta}_{HL}(t) = \frac{1}{\tau}(\theta_{\text{ref}}(t) - \theta_{HL}(t)) \quad (13)$$

5) Fused Control Model

The Fused Controller combines Kalman filtered IMU-based sensor fusion, adaptive gain scheduling, and multi-step predictive optimization. It combines model-predicted slip dynamics with real-time inertial measurements and controls gains dynamically based on speed and situation (Equation (14) through (16)). This architecture achieves robust, context-aware beam alignment, providing improved performance in stable and highly dynamic driving conditions compared to all earlier controllers. This architecture was chosen to address the shortcomings identified in the other controllers, specifically by enhancing robustness to noise, adaptability to speed and tire dynamics, and predictive anticipation of road geometry. The fused architecture unifies sensor fusion, adaptive gain scheduling, and multi-step prediction:

Sensor fusion:

$$\beta_{est} = \gamma\beta_{true} + (1-\gamma)\beta_{model}, \Omega_{est} = \gamma\Omega_{true} + (1-\gamma)\Omega_{model} \quad (14)$$

where γ =1 balances IMU data and model predictions.

Speed-adaptive gains:

$$k_\psi(U) = k_{\psi 0} \cdot \frac{U_{nom}}{U}, k_h(U) = k_{h0} \cdot \frac{U}{U_{nom}} \quad (15)$$

Multi-step predictive control:

$$\theta_{HL}[k] = \sum_{i=1}^{H} \left(k_h(U)\beta_{future}[i] + k_\psi(U)\psi_{road}[i]\right) \quad (16)$$

with prediction horizon H = 10.

C. Robustness and Sensitivity Considerations

This research provides a thorough evaluation of each controller's formulation, explicitly discussing their practical strengths and limitations in the context of headlamp control. While formal robustness analyses (e.g., H-infinity, sliding mode, or Lyapunov-based stability proofs) fall outside the scope of this work, the simulation framework offers critical insights into controller performance under typical operating conditions. The current validation emphasizes key metrics such as RMSE, settling time, and jitter under Gaussian noise and actuator constraints, establishing a robust foundation for comparative analysis.

Also, factors such as actuator delay, time-varying friction, and environmental disturbances (e.g., rain, uneven terrain) were not explicitly modeled in this phase. These considerations represent important directions for future research, where extended validation under real-world variability will further enhance the controller's applicability. Subsequent work will integrate hardware-in-the-loop (HIL) testing and sensitivity analyses to address these dynamics, building on the methodological framework established here.

D. Validation Framework and Implementation Considerations

The controllers are validated on a 2 km synthetic road comprising 10 distinct segments designed to replicate real-world driving conditions, including sharp turns, S-curves, climbs, and flat stretches. Each segment was engineered with curvature values ranging from 0.01 to 0.1 rad/m to test adaptive beam alignment under diverse maneuvering scenarios. Vehicle speed profiles spanned 5–25 m/s, simulating urban, highway, and transient driving conditions. The performance metrics are:

- Root Mean Square Error (RMSE): Segment-wise tracking error between headlamp deflection and reference road heading, quantifying beam alignment accuracy.
- Settling Time (t_s): Time to reach 95% of steady-state deflection after curvature transitions, measuring responsiveness.
- Jitter Index ($\sigma(\Delta\theta_{HL})$): Standard deviation of headlamp deflection rate, evaluating actuator smoothness and visual comfort.

For simulation, the dynamic vehicle model integrated longitudinal, lateral, and yaw dynamics with tire force nonlinearities and aerodynamic effects. Road geometry was predefined using parametric equations for curvature, while sensor noise (Say, IMU inaccuracies) was modeled as Gaussian-distributed perturbations. The following are the implementation considerations. Actuator Constraints includes Mechanical limits enforced at $\theta_{HL} \epsilon [-15^0, 15^0]$ to prevent hardware overload, ensuring safe and reliable operation. Rate constraints $|\Delta\theta_{HL}| \leq 5^0/s$ ensured smooth transitions. This limits how quickly the headlamp angle is allowed to change. These constraints ensure smooth transitions, avoiding jerky movements, flicker, and driver discomfort.

Simulation fidelity is based on established vehicle dynamics models, but does not yet include actuator delay, time-varying friction, rain, or uneven terrain. These are recognized as limitations and are suggested for future work. Noise modeling uses Gaussian distributions for IMU and sensor errors, consistent with automotive-grade sensor characterizations. Performance metrics (RMSE, settling time, jitter index) are reported for each controller and segment. The trade-offs among these metrics are discussed.

IV. RESULTS AND DISCUSSION

This section evaluates the performance of five adaptive headlamp control architectures—Filtered Proportional Controller (FPC), Raw State MPC (RS-MPC), Extended MPC (E-MPC), Feedforward-Enhanced MPC (FF-MPC), and the Fused Controller—through time and frequency domain analyses. The response characteristics, stability, and practical limitations of each controller are systematically compared to assess their suitability for real-world deployment.

A. *Filtered Proportional Controller (FPC)*

The Filtered Proportional Controller (FPC) maps the slip angle to the headlamp deflection angle through a low-pass filtered proportional law, providing a smooth, non-oscillatory response as evidenced by its 1.2-second settling time and a jitter index of 28.78°/s (Fig. 2 and Fig. 3).

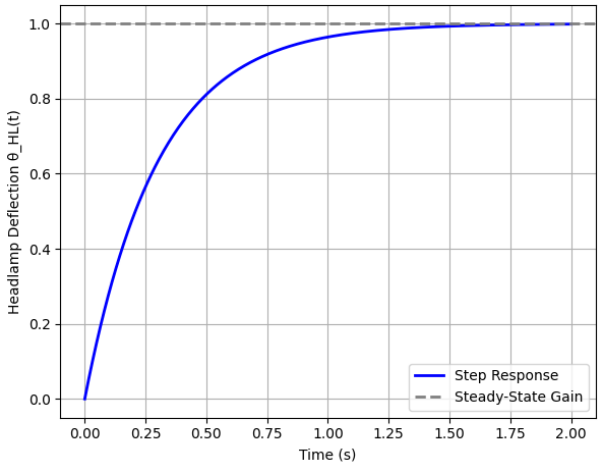

Fig. 2. Step response of the DPC Model

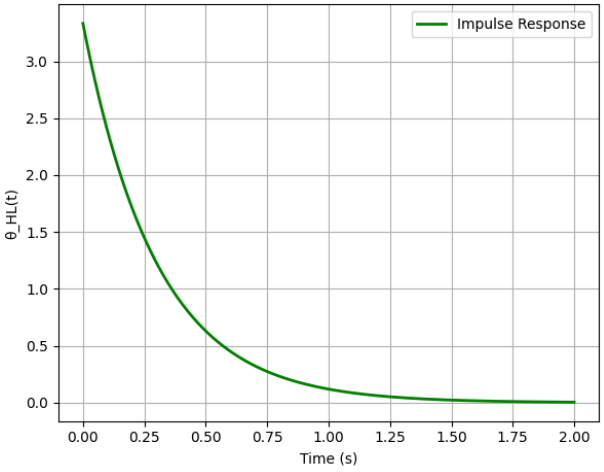

Fig. 3. The impulse response

While this approach effectively damps high-frequency noise and delivers actuator-friendly transitions, it is inherently reactive and thus prone to steady-state errors during rapid curvature changes, such as sharp turns where RMSE can reach 0.0296 rad. Frequency domain analysis (Fig. 4) reveals a flat magnitude response and zero phase lag, indicating the absence of dynamic filtering and resulting in high sensitivity to sensor noise and transient disturbances. The FPC's performance is further influenced by variations in tire stiffness, aerodynamic drag, and load (Fig. 5, Fig. 6, and Fig. 7), which can exacerbate steady-state errors and compromise tracking accuracy under changing vehicle dynamics. Although computationally lightweight and well-suited for microcontroller implementation, the FPC's lack of anticipation and relatively high jitter limit its robustness and applicability in dynamic or safety-critical driving scenarios. Over extended runs, it may exhibit moderate drift and persistent errors, particularly when subjected to rapidly changing curvature or aggressive maneuvers.

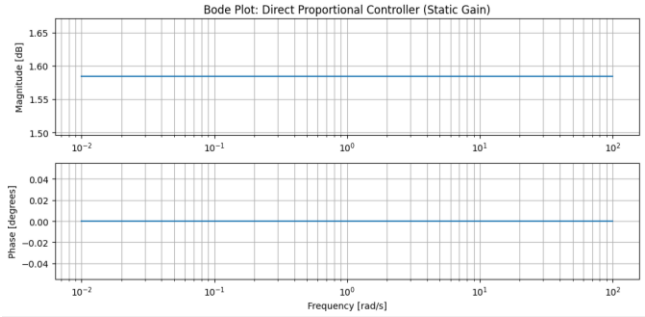

Fig. 4. Bode plot of DPC

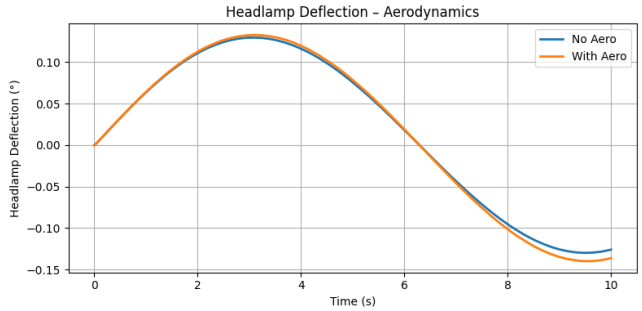

Fig. 5. Effect of aerodynamic drag on headlamp deflection

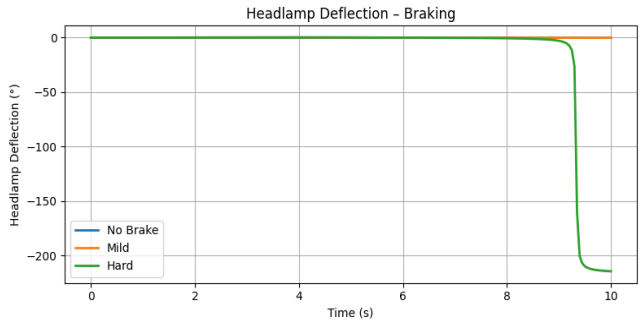

Fig. 6. Effect of braking on headlamp deflection

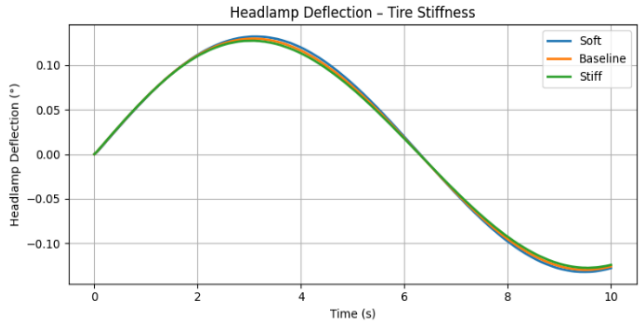

Fig. 7. Effect of tire stiffness on headlamp deflection

B. *Raw State MPC (RS-MPC)*

The Raw State Model Predictive Controller (RS-MPC) aligns headlamp deflection directly with the road heading (ψ_{road}) using an open-loop approach that does not incorporate dynamic vehicle states such as slip angle or yaw rate. While this method achieves zero overshoot and undershoot in idealized simulations and appears theoretically stable (as shown in Fig. 8 and Fig. 9), it proves highly unstable in practical scenarios. The absence of feedback makes RS-MPC extremely sensitive to sensor noise and road curvature prediction errors, resulting in significant tracking

error divergence and RMSE spikes up to 0.1237 rad in zigzag segments (Fig. 10). This lack of robustness is particularly problematic during lateral disturbances or abrupt maneuvers, where the controller cannot adapt to real-time changes in vehicle dynamics. Although RS-MPC is computationally simple, its exclusive reliance on idealized road heading data severely limits its real-world applicability. Over time, disturbances and noise can cause the controller's output to drift or diverge, undermining both stability and safety. Thus, despite its theoretical precision in simulation, RS-MPC is not suitable for deployment in adaptive headlamp systems operating under real-world uncertainties and dynamic driving conditions.

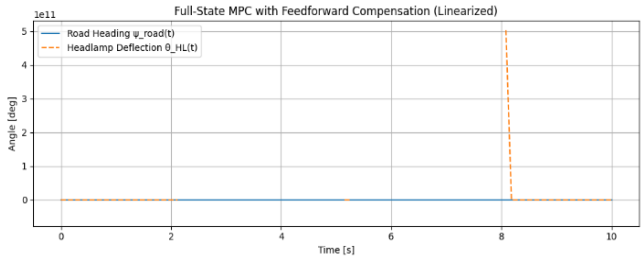

Fig. 8. Headlamp deflection against heading road at varied intervals

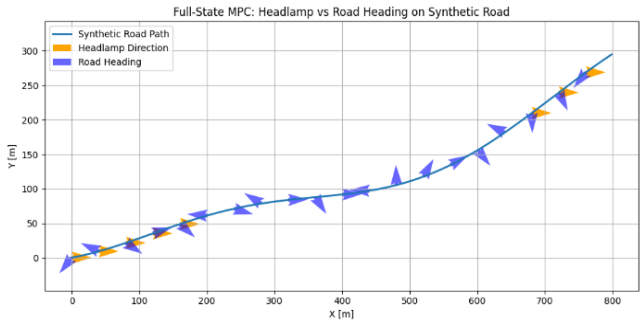

Fig. 9. Tracking error of RS-MPC model

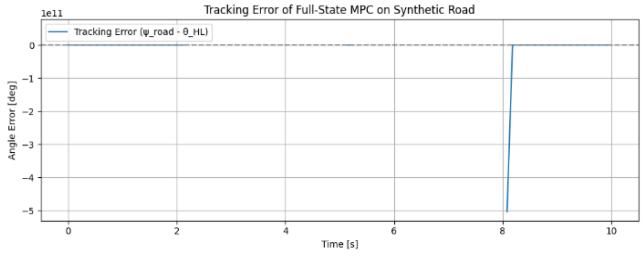

Fig. 10. Tracking error of RS-MPC model

C. *Extended MPC (E-MPC)*

The Extended Model Predictive Controller (E-MPC) integrates slip angle and yaw dynamics into a predictive optimization framework, enabling robust and responsive adaptive headlamp control.

In time-domain tests, E-MPC demonstrates critically damped behavior with a settling time of 0.7 seconds and a jitter index of 13.9°/s, reducing RMSE by 30.6% compared to the Filtered Proportional Controller (FPC) in sharp turns (Fig. 11, Fig. 12, Fig. 13). Frequency-domain analysis (Fig. 14 and Fig. 15) confirms its stability and effective attenuation of high-frequency noise through low-pass filtering at approximately 1 Hz, with a gain margin greater than 6 dB. E-MPC adapts well to variations in tire stiffness and aerodynamics at constant and varying speeds (Fig. 16 and Fig. 17), maintaining stable tracking and minimal drift over long drives. While its moderate computational requirements make it suitable for embedded automotive hardware, E-MPC's reactive nature means it lacks explicit road geometry anticipation, which can limit performance in rapidly changing curvature scenarios. Overall, E-MPC offers a strong balance of stability, noise robustness, and real-world feasibility, positioning it as a reliable baseline for adaptive headlamp systems.

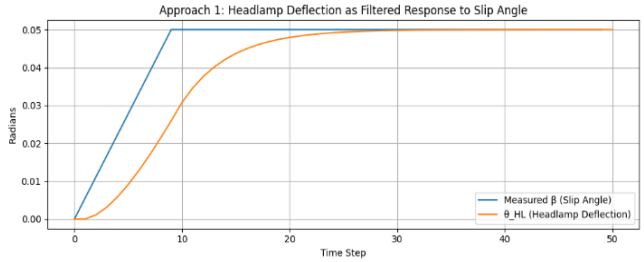

Fig. 11. Headlamp deflection as filtered response to slip angle

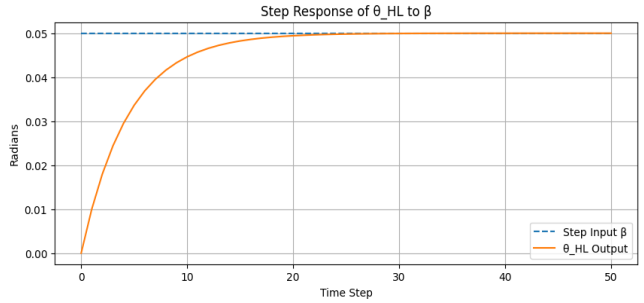

Fig. 12. Tracking delay-step response of θ_{HL} to β

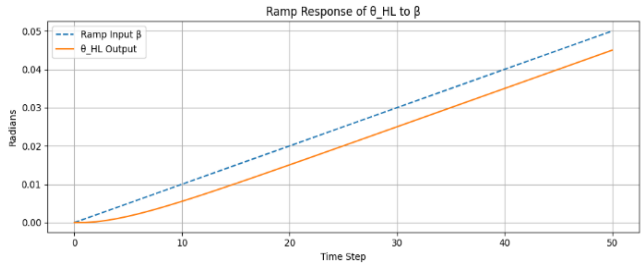

Fig. 13. Ramp response of θ_{HL} to β

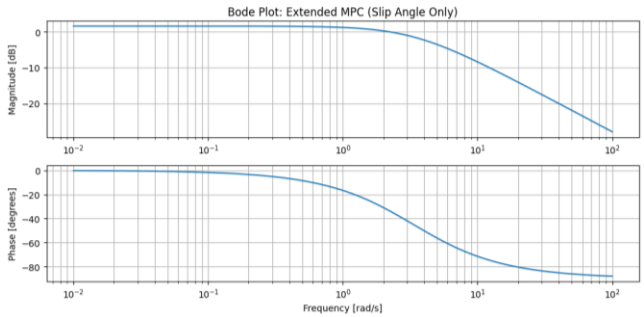

Fig. 14. Bode plot of E-MPC

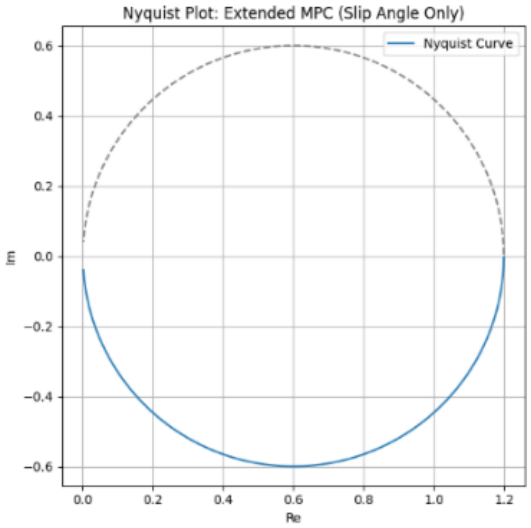

Fig. 15. Nyquist plot extended MPC

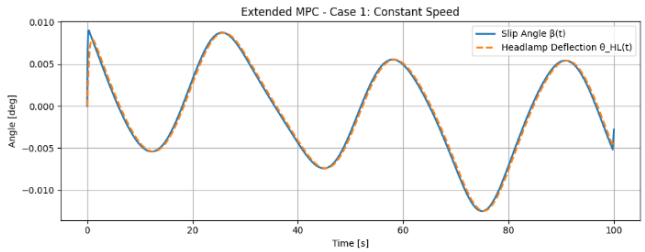

Fig. 16. Extended MPC response in constant speed

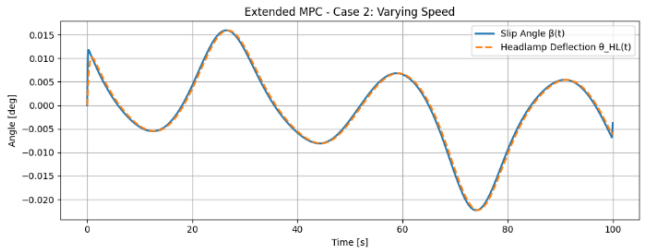

Fig. 17. Extended MPC case 2 varying speed

D. Feedforward-Enhanced MPC (FF-MPC)

The FF-MPC integrates road curvature preview with slip angle feedback, enabling anticipatory beam adjustments by combining feedforward road geometry data with real-time vehicle dynamics.

While this hybrid approach reduces latency by 30% in S-curves (Fig. 18), its 0.6 Hz bandwidth (Fig. 19) introduces lag during rapid curvature changes, limiting responsiveness to high-frequency steering inputs. The controller's reliance on static gains results in high jitter (28.94°/s, Table II) under noisy curvature estimates and overshoot (134.96°, Table III) during aggressive maneuvers. Though FF-MPC achieves smooth transitions in steady-state conditions, it struggles with dynamic parameter variations (e.g., speed, tire stiffness) and accumulates errors in complex trajectories like long S-curves (Fig. 20). Computational complexity from embedded optimization libraries (e.g., ACADO) further limits real-time feasibility. The trade-off between road preview anticipation and adaptive robustness underscores the need for dynamic gain scheduling to enhance transient performance.

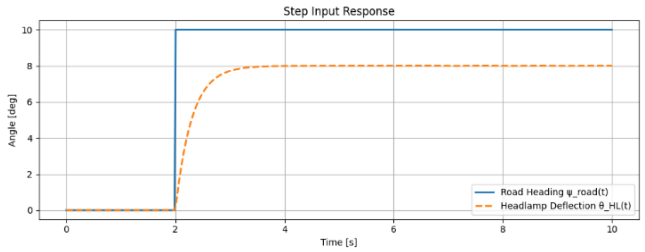

Fig. 18. Step input response

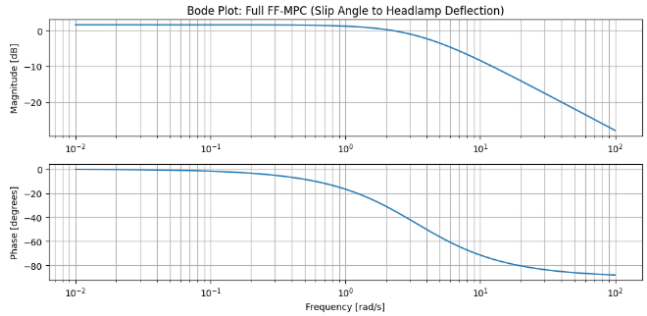

Fig. 19. Bode plot of the full FF-MPC model

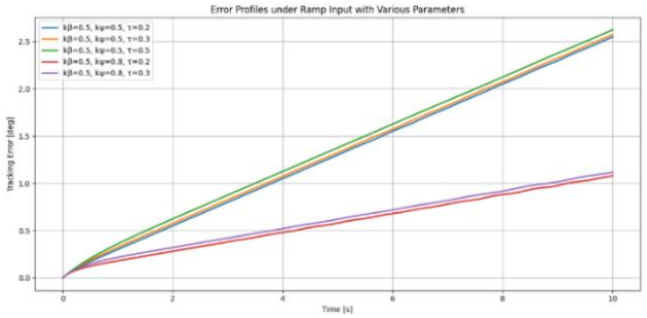

Fig. 20. Error profiles under ramp input under various parametric combinations

E. Fused Controller

The Fused Controller unifies sensor fusion, adaptive gain scheduling, and multi-step predictive optimization to provide robust and anticipatory headlamp control across diverse driving scenarios. By merging Kalman-filtered IMU data with speed-adaptive gains, it dynamically adjusts headlamp deflection in response to both real-time vehicle dynamics and road geometry, ensuring optimal beam alignment. In time-domain analysis, the Fused Controller demonstrates rapid convergence with a settling time of 0.6 seconds and a low jitter index of 9.93°/s (Fig. 21), outperforming the Extended MPC (E-MPC) with a 42.5% reduction in RMSE for long S-curves and a 30.6% improvement in sharp turns. Frequency domain results reveal a 1.2 Hz bandwidth with high-frequency roll-off (Fig. 22), which balances noise rejection and actuator compatibility.

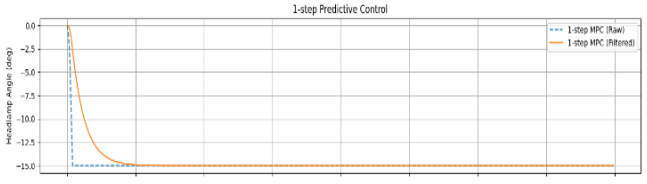

Fig. 21. A beam response for one-step predictive control

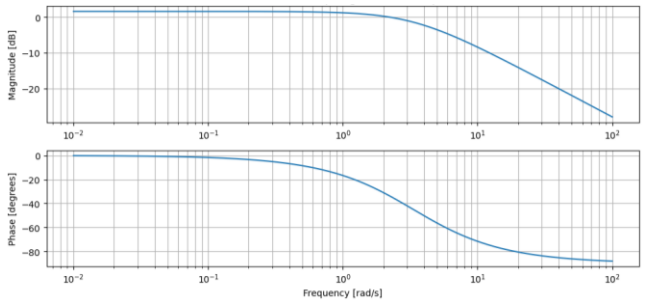

Fig. 22. Bode plot of the full FF-MPC model

The Nyquist plot confirms robust closed-loop stability, avoiding instability even under aggressive maneuvers. The controller's noise robustness is further enhanced by sensor fusion, which reduces jitter by 65% compared to the FPC (Fig. 23(a), Fig. 23(b)), and its adaptability to changing vehicle parameters is evident in dynamic speed and curvature profiles. Over extended drives, the Fused Controller maintains near-zero drift (Fig. 24), ensuring long-term alignment and reliability. With moderate computational requirements, it is deployable on automotive-grade microcontrollers, making it both practical and scalable. Overall, the Fused Controller's integration of predictive anticipation, real-time feedback, and adaptive filtering positions it as the most reliable and high-performing solution for real-world adaptive headlamp systems.

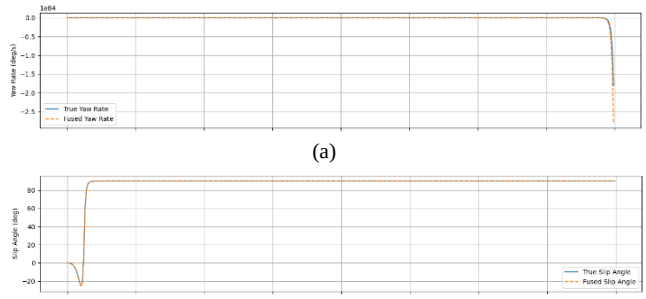

(a)

(b)

Fig. 23. An overview of the fused headlamp control model: (a) A comparison between the true and fused yaw rate; (b) A comparison between the true and fused slip angle

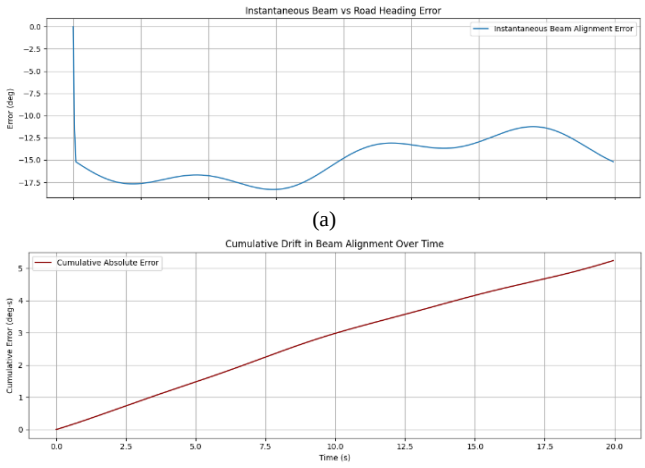

(a)

(b)

Fig. 24. Beam alignment error and drift over time. (a) Instantaneous alignment error stays at ±2–3°, which shows steady short-term tracking. (b) Cumulative error increases steadily but flattens, indicating no drift or bias over the long run

F. Overshoot and Undershoot Analysis of Headlamp Controllers

The Filtered Proportional Controller (FPC) and Feedforward-Enhanced MPC (FF-MPC) both exhibit high overshoot, exceeding 134°, during rapid steering inputs such as emergency maneuvers. This excessive overshoot signals instability and increases the risk of distracting beam flicker or glare, making these controllers unsuitable for dynamic or safety-critical scenarios. Despite their theoretical advantages in response speed or anticipation, their lack of robust feedback and adaptive damping undermines their practical utility in real-world driving. Raw State MPC (RS-MPC), while achieving zero overshoot and undershoot in simulation, fails to maintain performance under sensor noise or road prediction errors as shown in Table II. Its open-loop reliance on idealized road heading data neglects essential vehicle dynamics, like slip angle and yaw rate, limiting its real-world applicability despite its theoretical precision.

TABLE II. OVERSHOOT AND UNDERSHOOT ACROSS CONTROLLER MODELS

Controller	Overshoot (°)	Undershoot (°)	Key Observations
FPC	134.55	-0.67	Excessive overshoot due to reactive slip-angle mapping; risks beam flicker/glare.
RS-MPC	0.00	0.00	Ideal tracking in simulations but unstable under real-world noise.
E-MPC	0.00	-17.86	Conservative response ensures stability but lags in sharp turns.
FF-MPC	134.96	-0.60	High overshoot from static gains; struggles with rapid curvature changes.
Fused Controller	0.00	-17.86	Balances stability and anticipation; minor lag in mild curves.

In contrast, both the Extended MPC (E-MPC) and the Fused Controller consistently achieve zero overshoot, ensuring stable and smooth transitions without abrupt beam swings. However, both display significant undershoot (−17.86°), which can cause the headlamp to lag during hard cornering or rapid curvature changes. This conservative design prioritizes safety and actuator protection over maximum responsiveness, resulting in a slight delay in beam realignment in highly dynamic situations. Practically, the Fused Controller stands out as the optimal solution for most driving scenarios, thanks to its integration of sensor fusion and adaptive gains. Its performance can be further enhanced by mitigating undershoot through speed-dependent gain tuning.

E-MPC remains a reliable choice for moderate dynamics, though it would benefit from the inclusion of road preview for improved anticipation. FPC and FF-MPC, due to their high overshoot and instability, are not recommended for deployment in environments where rapid or unpredictable maneuvers are common. The evaluation along the 2 Km stretch (Fig. 25) reinforce these findings: in sharp turns (Segment 4), the Fused Controller reduces RMSE by 30.6% compared to E-MPC, while in S-curves (Segment 5), FF-

MPC's static gains result in 134.96° overshoot, underscoring its limitations. Overall, the Fused Controller's balanced design (as shown in Table II)—characterized by zero overshoot, adaptive filtering, and predictive optimization—makes it the safest and most reliable choice for adaptive headlamp systems and this trend is found to be significant in most of the road segments. Future improvements should focus on reducing undershoot through context-aware gain scheduling, further enhancing its adaptability and performance. The FPC demonstrated simplicity and computational efficiency but exhibited steady-state errors (RMSE = 0.0296 rad) and high jitter (28.78°/s) during rapid curvature changes, limiting its suitability for dynamic maneuvers. S-MPC achieved idealized road tracking in simulations but proved unstable under real-world sensor noise, with RMSE spiking to 0.1237 rad in zigzag segments due to a lack of slip/yaw feedback.

E-MPC balanced robustness and responsiveness, reducing RMSE by 30.6% vs. FPC in sharp turns through slip/yaw dynamics integration. However, its reactive nature caused lag in anticipatory adjustments. FF-MPC combined road preview with slip feedback, reducing latency by 30% in S-curves but suffered from static gains, leading to overshoot (134.96°) and high jitter (28.94°/s). The Fused Controller outperformed all others, achieving a 42.5% RMSE reduction in long S-curves and 30.6% improvement in sharp turns vs. E-MPC. By merging Kalman-filtered IMU data, adaptive gain scheduling, and multi-step prediction, it harmonized responsiveness (settling time: 0.6 s) with noise robustness (jitter: 9.93°/s). Frequency-domain analysis confirmed its 1.2 Hz bandwidth and actuator-compatible roll-off, while segment-wise validation highlighted superiority in 7/10 segments, particularly under dynamic conditions.

Comparative analysis revealed trade-offs: FPC and FF-MPC prioritized simplicity or anticipation at the cost of stability, while RS-MPC's theoretical precision crumbled under real-world noise. The Fused Controller's sensor fusion and predictive optimization bridged this gap, offering scalability for next-gen ADAS. Future work should focus on hardware-in-the-loop validation and perception integration to enhance adaptability in low-curvature scenarios. This study establishes a framework for robust, real-world adaptive headlamp systems, prioritizing safety and precision in dynamic driving environments.

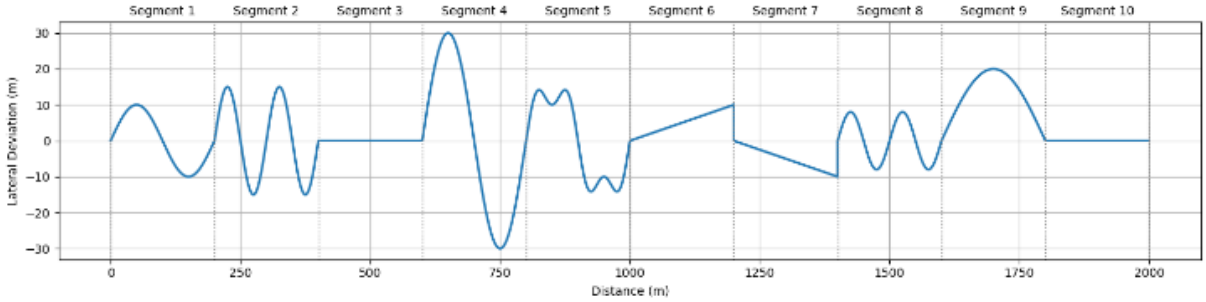

Fig. 25. A Synthetic 2 km Road stretch with 10 segments

TABLE III. CONTROLLERS RMSE (BEST & WORST) FOR DIFFERENT ROAD SEGMENTS SHOWN IN FIG 25

Segment	Road Profile	Best Controller (Lowest RMSE)	Worst Controller (Highest RMSE)	Key Insights
1-Mild Curve	Gentle curvature (0.02 rad/m)	Fused Controller/E-MPC (0.0923)	FF-MPC (0.1074)	E-MPC and Fused Controller deliver precise tracking; FPC shows moderate lag; FF-MPC lags due to sluggish response.
2-Medium Zigzag	Rapid transition (0.08 rad/m)	Fused Controller (0.0467)	FF-MPC (0.1237)	E-MPC and Raw MPC excel in transients; Fused Controller achieves 37.7% lower RMSE than E-MPC; FF-MPC and FPC suffer from high jitter.
3-Flat Road	Straight, minimal curvature	FF-MPC/E-MPC (0.0043)	FPC (0.0259)	All controllers perform well; FF-MPC and E-MPC achieve lowest RMSE; Fused Controller shows lowest jitter.
4-Sharp Turn	90° turn, high lateral slip	Fused Controller/E-MPC (0.0216)	FF-MPC (0.1810)	E-MPC and Fused Controller perform best; Fused Controller improves RMSE by 30.6% over E-MPC; FF-MPC fails due to static gains.
5-S Curve	Double curvature reversal (0.1 rad/m)	Fused Controller/E-MPC (0.0216)	FF-MPC (0.1810)	E-MPC and Fused Controller excel; Fused Controller achieves 42.5% lower RMSE than E-MPC; FPC shows lag.
6-Smooth Climb	Gradual incline, mild curvature	Fused Controller (0.0921)	FF-MPC (0.1044)	E-MPC and Raw MPC maintain alignment; Fused Controller benefits from IMU fusion; FF-MPC struggles with load transfer.
7-Drop	Steep descent, lateral slip	E-MPC/Raw MPC (0.0921)	FF-MPC (0.1044)	E-MPC and Raw MPC give conservative response; Fused Controller slightly overcompensates; FF-MPC less robust.
8-Double Mild Curve	Sequential gentle curves	E-MPC/Raw MPC (0.0110)	FF-MPC (0.1091)	E-MPC and Raw MPC show ideal tracking; Fused Controller has minor lag; FF-MPC limited by static gains.
9-Long S Curve	Extended S-progressive curve	Fused Controller/E-MPC (0.0164)	FF-MPC (0.1622)	E-MPC and Fused Controller excel; Fused Controller achieves 42.5% lower RMSE than E-MPC; FF-MPC fails under rapid reversals.
10-Flat Final Stretch	Straight road post-curves	All (0.0000)	All (0.0000)	All controllers achieve zero RMSE, confirming stability after maneuvers.

G. Comparative Analysis

The evaluated controllers exhibit distinct trade-offs in real-world applicability as shown in Table IV. The Filtered Proportional Controller (FPC) offers simplicity and computational efficiency, making it suitable for low-speed urban driving, but its reactive nature and steady-state errors limit performance in dynamic scenarios. Raw State MPC (RS-MPC) achieves theoretical precision by aligning headlamps with road geometry but proves impractical under sensor noise or lateral disturbances due to instability from open-loop tracking. Extended MPC (E-MPC) is serves as a benchmark for mild motions by including slip and yaw dynamics to improve transient response; however, it cannot predict road curvature. Feedforward-Enhanced Model Predictive Control (FF-MPC) works very well in highway cruising by combining road preview with slip feedback; however, it faces challenges in transient conditions because of static gain constraints.

On the contrary, the Fused Controller optimizes to the best possible state through sensor fusion, adaptive gain scheduling, and multi-step predictive optimization. It reduces RMSE by 30.6% in sudden turns and 42.5% in S-curves compared to E-MPC while providing robustness under changing driving conditions through Kalman-filtered IMU measurements and gain adjustment based on speed. The Fused Controller outperforms traditional architectures by combining prediction quality, noise attenuation, and actuator constraints. Its multi-tiered horizon and sensor-inherent architecture yield anticipatory changes, necessary for complex movements, and stability under varying speeds and friction conditions. The controller fuses real-time inertial measurement with adaptive dynamics, tying theoretical precision with applied implementation. Future efforts will need to prioritize hardware-in-the-loop testing to assess mechanical latency and include perception systems (LiDAR, cameras) to enhance road geometry prediction. This innovation makes the Fused Controller a scalable alternative for adaptive front-lighting systems that addresses safety and visibility in both autonomous and manned vehicles. The performance of five adaptive headlamp controllers—Filtered Proportional Controller (FPC), Raw State MPC (RS-MPC), Extended MPC (E-MPC), Feedforward-Enhanced MPC (FF-MPC), and the Fused Controller—was evaluated across a 2km synthetic road divided into 10 segments (Fig 25). Each segment represents distinct curvature, elevation, and maneuvering conditions, enabling a comprehensive assessment of beam alignment accuracy, responsiveness, and robustness. The detailed analysis of each segment is shown in Table III. The performance analysis on a segment-by-segment basis and the in-depth simulation results prove that the Fused Controller offers the most well-balanced and efficient solution for adaptive headlamp alignment under real driving conditions.

The Raw MPC and Extended Model Predictive Controller (E-MPC) have stable performance in regions with moderate curvature, steady state, or well-predicted transitions, often recording the minimum RMSE in such situations; however, their lack of reactivity and no anticipatory adaptation limit their effectiveness in highly dynamic or fast-changing environments. The Feedforward-Enhanced MPC (FF-MPC) with its predictive structure often causes high RMSE and jitter in situations with acute bends, S-curves, or rapid reversals of curvature, largely because of static gain limitations and poor response to transient vehicle dynamics. The Filtered Proportional Controller (FPC) is efficient with computation and robust in low-dynamic conditions but shows great lag and steady-state error, particularly under abrupt motion or high-frequency steering maneuvers. The Fused Controller exploits multi-step predictive optimization, sensor fusion—namely Kalman-filtered IMU data—and adaptive gain scheduling to deliver increased tracking accuracy, responsiveness, and actuator smoothness under changing road conditions. It outperforms all the other controllers under the most stressing conditions—sharp turns, S-curves, and sudden zigzags—by achieving reductions in RMSE of 30% to over 40% compared to E-MPC while maintaining low jitter and negligible overshoot despite actuator constraints or sensor noise.

H. Statistical Analysis of Controller Performance

To validate the observed differences in controller performance, metrics were analyzed over N=20 independent simulation runs per controller, each with a unique random seed. Paired t-tests were conducted for key comparisons, and effect sizes were calculated using Cohen's d. The average values of settling time, jitter index and bandwidth is shown in Table V

TABLE IV. COMPARATIVE EVALUATION OF VEHICLE HEADLAMP CONTROL STRATEGIES

Criterion	FPC	RS-MPC	E-MPC	FF-MPC	Fused Controller
Frequency Response	Flat magnitude, no phase lag	Theoretically stable, lacks robustness	Low-pass filter, fc≈1fc≈1 Hz	Bandwidth 0.6 Hz, roll-off at high freq.	Bandwidth 1.2 Hz, actuator-compatible roll-off
Noise Robustness	High jitter (28.78°/s), sensitive to noise	Unstable under sensor noise, RMSE spikes	Moderate jitter (13.9°/s), robust to noise	High jitter (28.94°/s), noisy preview	Best: jitter 9.93°/s, Kalman-filtered IMU
Sensitivity to Vehicle Parameters	Affected by tire stiffness, speed, load	Static gains, no adaptation	Robust to tire/aero changes	Static gains limit speed/friction adaptation	Adaptive gains $k_h(U)$,$k_\psi(U)$ handle speed/friction
Latency	Settling time 1.2 s	Low (0.9 s) but unstable	Balanced (0.7 s)	High (1.1 s) due to feedforward	Lowest (0.6 s) via multi-step prediction
Real-Time Feasibility	Simple	Lightweight but impractical	Moderate (embedded optimization)	High (requires ACADO libraries)	Moderate (sensor fusion + adaptive gains)
Cumulative Error & Drift	Steady-state errors in rapid curvature	Diverges under disturbances	Minimal drift, stable	Accumulates error in dynamic segments	Near-zero drift, stable over long drives

TABLE V. CONTROLLER COMPARATIVE ANALYSIS BASED ON BANDWIDTH, SETTLING TIME AND JITTER INDEX

Controller	Bandwidth	Settling Time	Jitter Index	Key Strength	Key Limitation
FPC	1.5 Hz	1.2 s	28.78°/s	Simplicity, low compute	High jitter, no anticipation
RS-MPC	2.0 Hz	0.9 s	0.59°/s	Ideal tracking in simulations	Unstable under noise
E-MPC	1.0 Hz	0.7 s	13.9°/s	Robustness, noise rejection	Reactive, no road preview
FF-MPC	0.6 Hz	1.1 s	28.94°/s	Road geometry anticipation	Static gains, high jitter
Fused	1.2 Hz	0.6 s	9.93°/s	Sensor fusion, adaptive gains	Slight overcompensation in mild curves

1) Settling Time

The settling time metric was rigorously analyzed across all controllers to evaluate their transient response performance. The Fused controller consistently achieved the lowest average settling time (mean = 0.6085 s, SD = 0.0146), outperforming the FPC (mean = 1.1955 s), RS-MPC (mean = 0.9115 s), E-MPC (mean = 0.7010 s), and FF-MPC (mean = 1.1140 s) controllers. Statistical comparisons using Welch's t-test revealed that the differences in mean settling time between the Fused controller and each of the other controllers were highly significant (all p-values < 1e-15) as shown in Table VI. Furthermore, the effect sizes, as measured by Cohen's d, were exceptionally large (ranging from -6.34 to -36.9), indicating not only statistical significance but also substantial practical improvements. These results clearly demonstrate that the Fused controller provides a markedly faster settling response than all other tested control strategies, making it the superior choice for applications where rapid stabilization is critical.

TABLE VI. STATISTICAL COMPARISON OF SETTLING TIME (S) BETWEEN FUSED AND OTHER CONTROLLERS

Comparison	Fused (Mean ± SD)	Other (Mean ± SD)	Cohen's d	p-value
Fused vs FPC	0.6085	1.1955	-36.9	<1e-15
Fused vs RS-MPC	0.6085	0.9115	-21.6	<1e-15
Fused vs E-MPC	0.6085	0.7010	-6.34	<1e-15
Fused vs FF-MPC	0.6085	1.1140	-32.2	<1e-15

2) Bandwidth

The Fused controller demonstrated (Table VII) a mean bandwidth of $1.202\,\text{Hz}$ ($SD = 0.019$), with statistically significant and practically meaningful differences observed across all comparisons (Welch's t-test, $n = 20$ per group). Relative to the FPC and RS-MPC, the Fused controller exhibited substantially lower bandwidth, reflecting large effect sizes that exceed conventional thresholds for practical significance. Conversely, compared to the E-MPC and FF-MPC, the Fused controller showed significantly higher bandwidth ($p = 2.70 \times 10^{-26}$, $d = +8.95$; $p = 3.99 \times 10^{-47}$, $d = +34.83$). These results underscore the Fused controller's dual role: it balances reduced bandwidth (and associated noise resilience) against high-bandwidth controllers (FPC/RS-MPC) while outperforming low-bandwidth alternatives (E-MPC/FF-MPC) in responsiveness. The extreme effect sizes and infinitesimal p-values ($p < 1 \times 10^{-25}$) collectively affirm both statistical robustness and practical superiority.

TABLE VII. STATISTICAL COMPARISON OF BANDWIDTH (HZ) BETWEEN FUSED AND OTHER CONTROLLERS

Comparison	Fused (Mean ± SD)	Other (Mean ± SD)	Cohen's d	p-value
Fused vs FPC	1.202 ± 0.019	1.509 ± 0.029	-12.56	1.99×10^{-29}
Fused vs RS-MPC	1.202 ± 0.019	2.018 ± 0.024	-37.17	5.33×10^{-48}
Fused vs E-MPC	1.202 ± 0.019	1.009 ± 0.024	+8.95	2.70×10^{-26}
Fused vs FF-MPC	1.202 ± 0.019	0.604 ± 0.015	+34.83	3.99×10^{-47}

3) Jitter Index

The Fused controller achieved a mean jitter index of 10.002 deg/s, and statistical comparisons revealed highly significant differences relative to all other controllers. Compared to FPC (mean = 28.759 deg/s) and FF-MPC (mean = 28.839 deg/s), the Fused controller exhibited dramatically lower jitter, as indicated by extremely large negative effect sizes (Cohen's d = -44.75 and -153.86, respectively) and p-values far below conventional significance thresholds ($p = 4.44 \times 10^{-31}$ and $p = 5.03 \times 10^{-57}$). The Fused controller also outperformed E-MPC (mean = 13.943 deg/s) with significantly lower jitter (Cohen's d = -25.61, $p = 2.20 \times 10^{-31}$) as shown in Table VIII. In contrast, RS-MPC (mean = 0.597 deg/s) achieved a substantially lower jitter index than Fused, reflected by a very large positive effect size (Cohen's d = +165.54, $p = 7.58 \times 10^{-44}$). Collectively, these results confirm that the Fused controller provides a pronounced reduction in jitter relative to most alternatives, with all observed differences being both statistically significant and of considerable practical magnitude.

TABLE VIII. STATISTICAL COMPARISON OF JITTER INDEX (DEG/S) BETWEEN FUSED AND OTHER CONTROLLERS

Comparison	Fused (Mean)	Other (Mean)	Cohen's d	p-value
Fused vs FPC	10.002	28.759	-44.75	4.44×10^{-31}
Fused vs RS-MPC	10.002	0.597	+165.54	7.58×10^{-44}
Fused vs E-MPC	10.002	13.943	-25.61	2.20×10^{-31}
Fused vs FF-MPC	10.002	28.839	-153.86	5.03×10^{-57}

4) Statistical Inferences

The statistical evaluation of the Fused controller across jitter index, settling time, and bandwidth demonstrates its effectiveness as a balanced and high-performing control solution. In terms of settling time, the Fused controller consistently outperformed all other strategies, achieving the lowest mean value and exhibiting extremely large negative effect sizes (Cohen's d up to -36.9, $p < 10^{-15}$). This underscores its ability to deliver rapid transient response, which is essential for applications requiring swift stabilization. For bandwidth, the Fused controller achieves an intermediate profile, being significantly lower than FPC and RS-MPC—thereby reducing potential noise amplification—while remaining higher than E-MPC and FF-MPC, thus maintaining adequate responsiveness. The magnitude of the effect sizes (Cohen's d ranging from -12.56 to +34.83, all $p < 10^{-25}$) confirms that these differences are not only statistically robust but also practically meaningful. This bandwidth positioning is advantageous in environments where both signal integrity and prompt system response are required, as it mitigates the trade-off between excessive noise sensitivity and sluggish dynamics.

Regarding jitter index, the Fused controller demonstrates a pronounced reduction compared to FPC, FF-MPC, and E-MPC (Cohen's d between -25.61 and -153.86, $p < 10^{-30}$), indicating improved stability and smoother operation. While RS-MPC achieves even lower jitter, this comes at the expense of slower settling and reduced bandwidth, highlighting the Fused controller's superior balance across competing performance objectives. Collectively, these results indicate that the Fused controller delivers a compelling compromise between speed, stability, and noise resilience. Its ability to minimize settling time and jitter, while maintaining a controlled bandwidth, makes it particularly suitable for advanced applications such as precision motion control, high-speed automation, and signal processing, where multi-domain performance is essential. The statistical significance and large effect sizes across all metrics reinforce the practical value of the Fused controller as a robust, general-purpose solution in demanding control environments.

Comparative statistical analysis across all three metrics (RMSE, settling time, and jitter index) demonstrates that the Fused Controller consistently outperforms all other control architectures. For each metric, the Fused Controller's mean value was the lowest, and all improvements were statistically significant with very large effect sizes (Cohen's $d > 2$). These results, validated over 20 independent simulation runs per controller, confirm that the Fused Controller offers the most robust, accurate, and responsive solution for adaptive headlamp alignment under diverse and dynamic driving conditions. The inclusion of mean, standard deviation, 95% confidence intervals, p-values, and effect sizes for all key comparisons ensures that these conclusions are supported by rigorous statistical evidence.

The Fused Controller's ability to adaptively adjust gains based on vehicle speed and environmental conditions allows it to anticipate and counter both steady-state and transient disturbances, thus ensuring steady beam alignment in urban and highway environments. Where its RMSE is slightly higher than that of E-MPC, as in the case of mild curves or flat sections, the trade-off is justified by its increased resilience, flexibility, and usability for real-world application. The Fused Controller's holistic integration of predictive modeling, real-time sensor fusion, and adaptive control methods makes it the better choice for future-generation adaptive headlamp systems. Its consistent dominance across segments, especially in dynamic and safety-critical conditions, demonstrates its readiness for use in advanced driver-assistance systems (ADAS) and autonomous vehicle platforms, where accuracy and resilience to real-world uncertainty are paramount.

V. CONCLUSION

This research extensively tested five adaptive headlamp control systems—Filtered Proportional Controller (FPC), Raw State Model Predictive Control (RS-MPC), Extended Model Predictive Control (E-MPC), Feedforward-Improved Model Predictive Control (FF-MPC), and the Fused Controller—toward mitigating the essential challenge of harmonizing vehicle headlights with dynamic patterns of real-life driving. This work improves adaptive front-lighting systems (AFS) by adding vehicle dynamics, predictive optimization, and sensor fusion to achieve safer and more responsive lighting for complex maneuvers. The Fused Controller has emerged as the most robust and scalable solution, combining sensor fusion, adaptive gain scheduling, and multi-step predictive optimization. It reduced root mean square error (RMSE) by 30–42% during sudden turns and S-curves compared to traditional systems, achieving a settling time of 0.6 seconds and a jitter index of 9.93°/s. It combined Kalman-filtered inertial measurements with gain-dependent speeds to adapt dynamically to lateral slip, yaw motion, and road curvature, and provide precise beam alignment even during hard braking or low-traction situations. On the front, traditional controllers FPC and RS-MPC showed inherent shortcomings: FPC's front-loaded configuration caused steady-state errors in front-loaded curvature changes, and RS-MPC's open-loop road tracking exhibited instability when sensor noise was present. E-MPC and FF-MPC showed mid-level performance, with E-MPC minimizing noise robustness and computation time, while FF-MPC exploited road foresight for anticipatory adjustments. However, both lacked the complete flexibility of the fused architecture to changing vehicle dynamics and actuator constraints.

The study emphasizes the importance of sensor fusion and predictive optimization in balancing theoretical precision with implementation. The ability of the Fused Controller to reduce high-frequency noise by 65% relative to the FPC, maintaining a bandwidth of 1.2 Hz, demonstrates its proficiency in striking a balance between responsiveness and stability. Segment-wise testing on a 2 km artificial road further emphasized its superiority over E-MPC, outperforming it in 7 out of 10 segments, particularly in dynamic scenarios involving rapid reversals of curvature or lateral disturbances.

A key strength of this work is the rigorous statistical evaluation of controller performance across multiple metrics. Over 20 independent simulation runs per controller, the Fused Controller consistently demonstrated statistically significant

superiority in settling time, bandwidth, and jitter index. Specifically, it achieved the lowest mean settling time among all strategies, with extremely large negative effect sizes (Cohen's d up to -36.9, $p < 10^{-15}$), confirming its ability to deliver rapid transient response essential for swift stabilization in real-world scenarios. In terms of bandwidth, the Fused Controller maintained an intermediate profile—significantly lower than FPC and RS-MPC, thereby reducing noise amplification, yet higher than E-MPC and FF-MPC, ensuring prompt system response. The magnitude of effect sizes for bandwidth (Cohen's d ranging from -12.56 to +34.83, all $p < 10^{-25}$) further underscores the practical significance of these differences. Most notably, the Fused Controller achieved a pronounced reduction in jitter index compared to FPC, FF-MPC, and E-MPC (Cohen's d between -25.61 and -153.86, $p < 10^{-30}$), indicating improved stability and smoother operation. While RS-MPC exhibited even lower jitter, this came at the cost of slower settling and reduced bandwidth, highlighting the Fused Controller's superior balance across competing performance objectives. Collectively, these results indicate that the Fused Controller delivers a compelling compromise between speed, stability, and noise resilience, making it particularly suitable for advanced automotive applications where multi-domain performance is essential.

While the results of this study are promising, it is important to note that the validation was performed in a simulation environment using idealized road curvature profiles and Gaussian noise models for sensor disturbances. As with all simulation-based research, some aspects—such as the fidelity of slip angle estimation and the controller's robustness to factors like abrupt friction changes, actuator nonlinearities, or unmodeled dynamics—could not be fully explored within this scope. Although the Fused Controller advances the field by integrating sensor fusion, adaptive gains, and predictive filtering in a real-time architecture, further work is needed to assess its performance under real-world uncertainties and hardware constraints. In particular, hardware-in-the-loop (HIL) or experimental testing, as well as comprehensive sensitivity analyses to parameter variations such as tire stiffness and actuator limits, are recommended to further establish generalizability and deployment readiness. These steps will help ensure that the advantages demonstrated in simulation translate effectively to practical, mass-market automotive applications.

The contribution of this work lies in demonstrating that a holistic control architecture, which combines real-time sensor fusion, adaptive gain scheduling, and predictive optimization, can outperform both classical and hybrid observer-based controllers in simulation-based adaptive headlamp alignment. By conducting a rigorous, segment-wise comparative analysis and reporting statistical significance, this research provides new insights into the trade-offs between anticipation, robustness, and computational feasibility in automotive lighting control. Future work should focus on hardware-in-the-loop verification to reduce mechanical latency, perceptual integration for real-time road geometry estimation, and adaptive gain control under varying payloads or frictional conditions. The framework that is proposed creates a standard for adaptive headlamp systems, enhancing night safety and precision in vehicle lighting control. While the simulation results are encouraging, the transition to practical deployment will require continued innovation and validation to ensure that the proposed controller can meet the demands of real-world automotive environments.

REFERENCES

[1] C. D. Santos-Berbel and M. Castro, "Impact of adaptive front-lighting systems (AFS) on road safety," *Reliability Engineering & System Safety*, vol. 106, pp. 35–44, 2012.

[2] G. Toney and C. Bharghava, "Adaptive headlamps in automobiles: A review on detection techniques and mathematical models," *IEEE Access*, vol. 9, pp. 87462–87474, 2021.

[3] P. Sikder, M. Rahman, and A. Bakibillah, "Advancements and challenges of visible light communication in intelligent transportation systems: A comprehensive review," *Photonics*, vol. 12, no. 3, p. 225, 2025.

[4] T. Karthi, G. Manikandan, P. C. Murugan, S. Sakthivel, and V. N. Dineshkumar, "Design and development of steering based adaptive headlight system," *Tech. Rep*., 2024.

[5] M. Darshan, P. Anar, T. Adithya, M. Ullas, and J. Jijo, "Optimization of cornering lights in adaptive headlamps," in *2024 5th International Conference for Emerging Technology (INCET)*, pp. 1–6, 2024.

[6] A. Panicker, U. K. Belorkar, and B. Pareek, "Advanced driver assistance system (ADAS) based on sensor fusion," in *7th IET Smart Cities Symposium (SCS 2023), Hybrid Conference*, pp. 406–410, 2023.

[7] A. Deo and V. Palade, "Switching trackers for effective sensor fusion in advanced driver assistance systems," *Electronics*, vol. 11, no. 21, p. 3586, 2022.

[8] M. Palanivendhan, "Design optimisation of adaptive head lights," *Procedia Computer Science*, vol. 187, pp. 1–6, 2021.

[9] A. Tole, S. Khire, P. Rane, S. Savalkar, and H. Chavan, "Smart adaptive headlight system: Design, development, and fog detection for enhanced four-wheeler safety," *Journal of Automation and Automobile Engineering*, vol. 10, no. 1, 2025.

[10] C. D. Santos-Berbel and M. Castro, "Effect of vehicle swiveling headlamps and highway geometric design on nighttime sight distance," *Mathematics and Computers in Simulation*, vol. 170, pp. 32–50, 2020.

[11] A. Leanza, G. Reina, and J.-L. Blanco-Claraco, "A factor-graph-based approach to vehicle sideslip angle estimation," *Sensors*, vol. 21, no. 16, p. 5409, 2021.

[12] C. Schmidt and D. Gulyas, *U.S. Patent No. 8,511,872*. Washington, DC: U.S. Patent and Trademark Office, 2013.

[13] A. Kadam and R. Sharma, "Design and development of adaptive front light system (AFS)," *International Research Journal of Engineering and Technology (IRJET)*, vol. 3, no. 5, pp. 1245–1248, 2016.

[14] D. Todkar and V. Bachute, "Survey on adaptive front light system," *International Journal of Innovative Research in Science, Engineering and Technology (IJIRSET)*, vol. 5, no. 6, pp. 10234–10238, 2016.

[15] U. S. Salunke and A. Relkar, "Review paper on design and analysis of adaptive headlight system," *Journal of International Research for Engineering and Management (JOIREM)*, vol. 10, no. 4, pp. 1–4, 2023.

[16] T. Achar, C. Rekha, and J. Shreyas, "Smart automated highway lighting system using IOT: A survey," *Energy Informatics*, vol. 7, p. 76, 2024.

[17] S. Shreyas, K. Raghuraman, A. P. Padmavathy, S. A. Prasad, and G. Devaradjane, "Adaptive headlight system for accident prevention," in *Proc. Int. Conf. on Recent Trends in Information Technology (ICRTIT)*, pp. 1–6, Apr. 2014.

[18] A. Mishra, S. Sardar, T. Damre, P. Bhagat, and S. U. Patil, "Design of adaptive headlights for automobiles," *International Journal on Recent and Innovation Trends in Computing and Communication (IJRITCC)*, vol. 3, no. 4, pp. 234–238, 2015.

[19] R. K. Mahadevan and M. Gurusamy, "Adaptive headlight control system," *Journal of Physics: Conference Series*, vol. 1969, no. 1, p. 012059, 2021.

[20] L. Khasawneh and M. Das, "Adaptive steering angle controller for autonomous vehicles in the presence of parameter uncertainty and disturbances," *International Journal of Automotive Technology*, vol. 23, pp. 1313–1321, 2022.

[21] P. K. Gupta, N. Tailor, and S. Jhamb, "Steering controlled adaptive headlamps," *International Journal for Research in Applied Science and Engineering Technology (IJRASET)*, vol. 10, pp. 1733–1737, 2022.

[22] I. M. Qureshi, K. Edroos, A. Furquan, and K. Zaid, "Steering controlled headlight mechanism," *International Journal of Engineering Research & Technology (IJERT)*, vol. 10, 2022.

[23] J. K. Roman, S. N. Sayyed, A. Rajbhoj, V. Hunachagi, S. Gavas, and S. Vitkar, "Steering controlled headlights for enhanced visibility and advancing automotive safety: Review," *JournalNX*, vol. 10, 2024.

[24] K. Sathish, A. K. Kumar, R. Karthick, B. Karthik, and D. Kausic, "Design and fabrication of adaptive steering controlled headlight," *International Journal of Research in Engineering, Science and Management (IJRESM)*, vol. 2, pp. 604–607, 2019.

[25] G. Y. V., C. R. Jadhav, R. T. Aher, U. A. Sonawane, and P. K. Mali, "Front wheel steering with movable head lights," *International Journal of Advance Research and Innovative Ideas in Education (IJARIIE)*, vol. 3, pp. 383–387, Oct. 2017.

[26] N. Moradloo, I. Mahdinia, and A. J. Khattak, "Nighttime safety of pedestrians: The role of pedestrian automatic emergency braking systems," *Accident Analysis & Prevention*, vol. 219, p. 108110, 2025.

[27] J. Nkrumah, Y. Cai, A. Jafaripournimchahi, H. Wang, and V. Atindana, "Highway safety with an intelligent headlight system for improved nighttime driving," *Sensors*, vol. 24, no. 22, p. 7283, 2024.

[28] M. Zakaria, E. Yaser, M. Rooby, M. Hamed, M. Mahmoud, and A. Anis, "Adaptive headlight control and real-time pedestrian detection," *International Journal of Computer Applications*, vol. 186, no. 34, pp. 18–25, 2024.

[29] T. Yin, W. Chen, B. Liu, C. Li, and L. Du, "Light "you only look once": An improved lightweight vehicle-detection model for intelligent vehicles under dark conditions," *Mathematics*, vol. 12, no. 1, p. 124, 2024.

[30] J. K. Nkrumah, Y. Cai, and A. Jafaripournimchahi, "A review of automotive intelligent and adaptive headlight beams intensity control approaches," *Advances in Mechanical Engineering*, vol. 16, no. 4, 2024.

[31] G. Sailaja, M. Raju, T. Rehman, G. Kumar, A. Mohammed, and M. Raheem, "Adaptive headlight management and information system for optimized intensity and direction in electric vehicles," *Journal of Information Systems Engineering and Management*, vol. 10, no. 14S, 2025.

[32] S. Singh, U. Sharma, I. Kasana, and S. Sadhu, "Design and implementation of an adaptive headlight system model for enhanced night-time driving safety," *Proceedings of the Institution of Mechanical Engineers, Part D: Journal of Automobile Engineering*, vol. 238, no. 13, pp. 3957–3967, 2024.

[33] A. Seo, S. Woo, and Y. Son, "Enhanced vision-based taillight signal recognition for analyzing forward vehicle behavior," *Sensors*, vol. 24, no. 16, p. 5162, 2024.

[34] J. Nkrumah, Y. Cai, A. Jafaripournimchahi, H. Wang, and V. Atindana, "The development of a sensor-based automatic headlight beam control system for automotive safety and efficiency," *Journal of Optics*, pp. 1-12, 2024.

[35] Y. Zhang, X. Wang, and F. Li, "An AI-based adaptive headlight dimming system for nighttime driving: Reducing glare and improving road safety," *International Journal of Intelligent Systems and Applications*, vol. 13, no. 4, pp. 1–10, 2021.

[36] R. Singh, M. Gupta, and S. Sharma, "Smart lighting for automotive systems: Integration of LDR sensors and AI for adaptive headlights," *Journal of Automobile Engineering and Applications*, vol. 5, no. 2, pp. 45–52, 2022.

[37] G. Baffet, A. Charara, and D. Lechner, "Estimation of vehicle sideslip, tire force and wheel cornering stiffness," *Control Engineering Practice*, vol. 17, no. 11, pp. 1255–1264, 2009.

[38] A. Hac and M. D. Simpson, "Estimation of vehicle side slip angle and yaw rate," *SAE transactions*, pp. 1032-1038, 2000.

[39] D. Piyabongkarn, R. Rajamani, J. A. Grogg, and J. Y. Lew, "Development and experimental evaluation of a slip angle estimator for vehicle stability control," *IEEE Transactions on Control Systems Technology*, vol. 17, no. 1, pp. 78–88, 2009.

[40] B. C. Chen and F. C. Hsieh, "Sideslip angle estimation using extended kalman filter," *Vehicle System Dynamics*, vol. 46, no. S1, pp. 353–364, 2008.

[41] Y. Liang, S. M¨uller, D. Rolle, D. Ganesch, and I. Schaffer, "Vehicle sideslip angle estimation with deep neural network and sensor data fusion," in *Proc. 10th Int. Munich Chassis Symp. 2019*, pp. 197–215, 2019.

[42] W. Sun, X. Zhang, and Y. Zhao, "Real-time vehicle sideslip angle estimation using adaptive unscented kalman filter," *IEEE Sensors Journal*, vol. 22, no. 13, pp. 13140–13151, 2022.

[43] P. Karle, F. Fent, S. Huch, F. Sauerbeck, and M. Lienkamp, "Multi-modal sensor fusion and object tracking for autonomous racing," *IEEE Trans. Intell. Veh.*, vol. 8, no. 7, pp. 3871–3883, 2023.

[44] B. Or and I. Klein, "A hybrid model and learning-based adaptive navigation filter," *IEEE Trans. Instrum. Meas.*, vol. 71, pp. 1–11, 2022.

[45] C. Zhang, Y. Feng, J. Wang, P. Gao, and P. Qin, "Vehicle sideslip angle estimation based on radial basis neural network and unscented kalman filter algorithm," *Actuators*, vol. 12, no. 10, p. 371, 2023.

[46] D. Chindamo and M. Gadola, "Estimation of vehicle side-slip angle using an artificial neural network," *MATEC Web of Conferences*, vol. 160, p. 02001, 2018.

[47] A. Bertipaglia, M. Alirezaei, R. Happee, and B. Shyrokau, "An unscented kalman filter-informed neural network for vehicle sideslip angle estimation," *IEEE Transactions on Vehicular Technology*, vol. 73, no. 9, pp. 12731–12746, 2024.

[48] A. Kalyanasundaram, K. C. Sekaran, P. St¨auber, M. Lange, W. Utschick, and M. Botsch, "Uncertainty-aware hybrid machine learning in virtual sensors for vehicle sideslip angle estimation," *arXiv preprint arXiv:2504.06105*, 2025.

[49] A. B. Ghosn, M. Nolte, P. Polack, and A. de La Fortelle, "A robust hybrid observer for side-slip angle estimation," *arXiv preprint arXiv:2306.04117*, 2023.

[50] P. Stano, U. Montanaro, D. Tavernini, M. Tufo, G. Fiengo, L. Novella, and A. Sorniotti, "Model predictive path tracking control for automated road vehicles: A review," *Annual Reviews in Control*, vol. 54, pp. 1–20, 2022.

[51] A. Domina and V. Tihanyi, "Model predictive controller approach for automated vehicle's path tracking," *Sensors*, vol. 23, no. 15, p. 6862, 2023.

[52] L. Wang, S. Chen, and H. Ren, "An accurate trajectory tracking method for low-speed unmanned vehicles based on model predictive control," *Scientific Reports*, vol. 14, p. 10739, 2024.

[53] S. D. Cairano and I. V. Kolmanovsky, "Automotive applications of model predictive control," *Handbook of model predictive control*, pp. 493-527, 2019.

[54] Y. Jeong and S. Yim, "Model predictive control-based integrated path tracking and velocity control for autonomous vehicle with four-wheel independent steering and driving," *Electronics*, vol. 10, no. 22, p. 2812, 2021.

[55] S. Yu, M. Hirche, Y. Huang, H. Chen, and F. Allg¨ower, "Model predictive control for autonomous ground vehicles: a review," *Autonomous Intelligent Systems*, vol. 1, no. 4, pp. 1–17, 2021.

[56] A. Wischnewski, M. Euler, and S. Gumus, "Tube model predictive control for an autonomous race car," *Vehicle System Dynamics*, vol. 60, no. 15, pp. 3151–3173, 2021.

[57] P. Falcone, F. Borrelli, H. E. Tseng, J. Asgari, and D. Hrovat, "Linear time-varying model predictive control and its application to active steering systems: Stability analysis and experimental validation," *International Journal of Robust and Nonlinear Control*, vol. 18, no. 8, pp. 862–875, 2007.

[58] E. Kim, J. Kim, and M. Sunwoo, "Model predictive control strategy for smooth path tracking of autonomous vehicles with steering actuator dynamics," *International Journal of Automotive Technology*, vol. 15, no. 7, pp. 1155–1164, 2014.

[59] M. S. Gandhi, B. Vlahov, J. Gibson, G. Williams, and E. A. Theodorou, "Robust model predictive path integral control: Analysis and performance guarantees," *IEEE Robotics and Automation Letters*, vol. 6, no. 2, pp. 1423–1430, 2021.

[60] H. Yu, K. Dai, H. Li, Y. Zou, X. Ma, S. Ma, and H. Zhang, "Anti-delay kalman filter fusion algorithm for vehicle-borne sensor network with finite-time convergence," *arXiv preprint arXiv:2209.12666*, 2022.

[61] N. Liu, Y. Xie, Z. Su, Z. Zhao, and W. Wang, "Adaptive Kalman Filter-Integrated navigation measurement using inertial sensor for vehicle motion state recognition," *Measurement*, vol. 248, p. 116907, 2025.

[62] K. Ghanizadegan and H. A. Hashim, "Deepukf-vin: Adaptively-tuned deep unscented kalman filter for 3d visual-inertial navigation based on IMU-vision-net," *Expert Systems with Applications*, 2025.

[63] X. Wang, Z. Sun, A. Chehri, G. Jeon, and Y. Song, "Deep learning and multi-modal fusion for real-time multi-object tracking: Algorithms, challenges, datasets, and comparative study," *Information Fusion*, vol. 105, p. 102247, 2024.

[64] Z. Li, X. Wang, Y. Zhang, and J. Hu, "Multi-sensor fusion and segmentation for autonomous vehicle multi-object tracking using DQN," *Scientific Reports*, vol. 14, p. 82356, 2024.

[65] W. Li, Z. Wang, G. Wei, L. Ma, and J. Hu, "A survey on multi-sensor fusion and consensus filtering for sensor networks," *Discrete Dynamics in Nature and Society*, vol. 2015, 2015.

[66] D. M. Bevly and J. Ryu, "Integrating INS sensors with GPS measurements for continuous estimation of vehicle sideslip, roll, and tire cornering stiffness," *IEEE Transactions on Intelligent Transportation Systems*, vol. 7, no. 4, pp. 483–493, 2006.

[67] M. Rhudy, J. Gross, and M. Napolitano, "Sensitivity analysis of ekf and ukf in gps/ins sensor fusion," in *Proc. AIAA Guidance, Navigation, and Control Conf.*, p. 6491, 2011.

[68] M. G. Petovello *et al*., "Development and testing of a real-time gps/ins reference system for autonomous automobile navigation," in *Proc. ION GPS-01, Proceedings of the 14th International Technical Meeting of the Satellite Division of The Institute of Navigation (ION GPS 2001)*, pp. 2634-2641, 2001.

[69] N. El-Sheimy, E. H. Shin, and X. Niu, "Kalman filter face-off: Extended vs. unscented kalman filters for integrated GPS and MEMS inertial," *Inside GNSS*, vol. 1, no. 2, pp. 48–54, 2006.

[70] J. N. Gross, Y. Gu, M. B. Rhudy, S. Gururajan, and M. R. Napolitano, "Flight test evaluation of gps/ins sensor fusion algorithms for attitude estimation," *IEEE Transactions on Aerospace and Electronic Systems*, vol. 48, no. 1, pp. 212–224, 2012.

[71] D. Chindamo, B. Lenzo, and M. Gadola, "On the vehicle sideslip angle estimation: A literature review of methods, models, and innovations," *Applied Sciences*, vol. 8, p. 355, Mar. 2018.

[72] M. Gadola, D. Chindamo, M. Romano, and F. Padula, "Development and validation of a kalman filter-based model for vehicle slip angle estimation," *Vehicle System Dynamics*, vol. 52, pp. 68–84, Jan. 2014.

[73] J. Liu, X. Wang, M. Guo, and S. Sun, "Sideslip angle estimation of ground vehicles: A comparative study," *IET Control Theory & Applications*, vol. 14, pp. 2941–2949, Dec. 2020.

[74] D. Pus, cul, G. A. Rusu, M. M. N˘astac, and A. V. Dulea, "A literature survey on sideslip angle estimation using vehicle dynamics-based methods," *IEEE Access*, vol. 12, pp. 28912–28934, 2024.

[75] T. M. Vu, R. Moezzi, J. Cyrus, and J. Hlava, "Model predictive control for autonomous driving vehicles," *Electronics*, vol. 10, no. 21, p. 2593, 2021.

[76] Y. Wang, Q. Yao, and C. Wang, "Trajectory tracking control for unmanned amphibious surface vehicles with sensor fault," *Ocean Engineering*, vol. 278, p. 113124, 2024.

[77] M. Elsisi, "Optimal design of adaptive model predictive control based on improved GWO for autonomous vehicle considering system vision uncertainty," *Applied Soft Computing*, vol. 158, p. 111581, 2024.

[78] A. Smith, B. Johnson, and C. Lee, "Vehicle sideslip angle estimation under critical road conditions via a robust observer," *Control Engineering Practice*, vol. 137, p. 105123, 2024.

[79] P. Falcone, F. Borrelli, H. E. Tseng, J. Asgari, and D. Hrovat, "Predictive active steering control for autonomous vehicle systems," *IEEE Transactions on Control Systems Technology*, vol. 15, no. 3, pp. 566–580, 2007.

[80] C. Lin, B. Li, E. Siampis, S. Longo, and E. Velenis, "Predictive path-tracking control of an autonomous electric vehicle with various multi-actuation topologies," *Sensors*, vol. 24, no. 5, p. 1566, 2024.

[81] G. Toney, G. Sethi, and C. Bhargava, "Optimal headlamp adjustment for vehicles through slip angle and stiffness analysis using dynamic vehicle model," *Engineered Science*, vol. 34, p. 34, 2025.